

# 1 Reconciling the Cretaceous breakup and demise of the Phoenix 2 Plate with East Gondwana orogenesis in New Zealand

3

4 Suzanna H.A. van de Lagemaat<sup>1,\*</sup>, Peter J.J. Kamp<sup>2</sup>, Lydian M. Boschman<sup>1</sup>, Douwe J.J. van  
5 Hinsbergen<sup>1</sup>

6

7 <sup>1</sup> Department of Earth Sciences, Utrecht University, Utrecht, the Netherlands

8 <sup>2</sup> School of Science, University of Waikato, Hamilton, New Zealand

9

10 \* Corresponding author: Suzanna van de Lagemaat (s.h.a.vandelagemaat@uu.nl)

11

## 12 **Highlights**

- 13 - GPlates reconstruction of the South Pacific realm back to 150 Ma
- 14 - Pacific Plate-Zealandia convergence continued until 90-85 Ma
- 15 - Subduction along the Zealandia margin may have continued until 79 Ma accommodated  
16 by Osbourn Trough spreading
- 17 - Reconstruction reveals ridge subduction rather than subduction termination as possible  
18 cause of a 105-100 Ma change in magmatic arc signature in Zealandia

19

20 **Keywords:** East Gondwana subduction zone, plate tectonics, GPlates, kinematic plate  
21 reconstruction, New Zealand, New Caledonia, Zealandia

22

23 **This paper is a non-peer reviewed manuscript submitted to EarthArXiv. The manuscript**  
24 **has been submitted for peer review to *Earth-Science Reviews***

25 **Abstract**

26 Following hundreds of millions of years of subduction in all circum-Pacific margins, the Pacific  
27 Plate started to share a mid-ocean ridge connection with continental Antarctica during a Late  
28 Cretaceous south Pacific plate reorganization. This reorganization was associated with the  
29 cessation of subduction of the remnants of the Phoenix Plate along the Zealandia margin of East  
30 Gondwana, but estimates for the age of this cessation from global plate reconstructions (~86  
31 Ma) are significantly younger than those based on overriding plate geological records (105-100  
32 Ma). To find where this discrepancy comes from, we first evaluate whether incorporating the  
33 latest available marine magnetic anomaly interpretations change the plate kinematic estimate  
34 for the end of convergence. We then identify ways to reconcile the outcome of the  
35 reconstruction with geological records of subduction along the Gondwana margin of New  
36 Zealand and New Caledonia. We focus on the plate kinematic evolution of the Phoenix Plate  
37 from 150 Ma onward, from its original spreading relative to the Pacific Plate, through its break-  
38 up during emplacement of the Ontong Java Nui Large Igneous Province into four plates  
39 (Manihiki, Hikurangi, Chasca, and Aluk), through to the end of their subduction below East  
40 Gondwana, to today. Our updated reconstruction is in line with previous compilations in  
41 demonstrating that as much as 800-1100 km of convergence occurred between the Pacific Plate  
42 and Zealandia after 100 Ma, which was accommodated until 90-85 Ma. Even more convergence  
43 occurred at the New Zealand sector owing to spreading of the Hikurangi Plate relative to the  
44 Pacific Plate at the Osbourn Trough, with the most recent age constraints suggesting that  
45 spreading may have continued until 79 Ma. The end of subduction below most of East  
46 Gondwana coincides with a change in relative plate motion between the Pacific Plate and East  
47 Gondwana from westerly to northerly, of which the cause remains unknown. In addition, the  
48 arrival of the Hikurangi Plateau in the subduction zone occurred independent from, and did not  
49 likely cause, the change in Pacific Plate motion. Finally, our plate reconstruction suggests that  
50 the previously identified geochemical change in the New Zealand arc around 105-100 Ma that  
51 was considered evidence of subduction cessation, may have been caused by Aluk-Hikurangi  
52 ridge subduction instead. The final stages of convergence before subduction cessation must  
53 have been accommodated by subduction without or with less accretion. This is common in  
54 oceanic subduction zones but makes dating the cessation of subduction from geological records  
55 alone challenging.

## 56 **1. Introduction**

57           During the Late Cretaceous, an important tectonic change occurred in the southern  
58 Pacific realm. For hundreds of millions of years, including most of the Mesozoic, the Panthalassa  
59 (or Paleo-Pacific) Ocean was surrounded by subduction zones that consumed oceanic  
60 lithosphere of the Farallon (NE), Izanagi (NW), and Phoenix (S) plates (e.g., Engebretson et al.  
61 1985; Seton et al., 2012; Wright et al., 2016; Müller et al., 2019; Torsvik et al., 2019; Boschman  
62 et al., 2021a). During the Cretaceous, however, subduction ended along the Zealandia sector of  
63 the East Gondwana continental margin (e.g., Bradshaw, 1989; Luyendyk, 1995; Davy et al.,  
64 2008; Matthews et al., 2012). Sections of the suture of the Mesozoic subduction zone are located  
65 along the northern margin of the Chatham Rise and along the Thurston Island sector of  
66 Antarctica, which are presently separated from each other by the Pacific-Antarctic Ridge (Fig.  
67 1). This implies that when Pacific-Antarctic spreading started, the ridge did not simply replace  
68 the former East Gondwana subduction zone. Instead, it cut through the subduction zone suture  
69 and formed partly intra-oceanic and partly intra-continental within East Gondwana lithosphere  
70 (Larter et al., 2002; Wobbe et al., 2012). Around the time of subduction cessation, several  
71 oceanic plates that formed after breakup of the Phoenix Plate, as well as part of Zealandia,  
72 merged with the Pacific Plate. Since then, the Pacific Plate has been diverging from West  
73 Antarctica, accommodated by oceanic spreading at the Pacific-Antarctic Ridge (Fig. 1B). But  
74 despite its importance in the plate tectonic history of the Panthalassa/Pacific domain, the  
75 southwest Pacific-East Gondwana plate reorganization is surrounded with uncertainty.

76           This uncertainty results from a discrepancy in the age of subduction cessation between  
77 different studies. On the one hand, geologists studying the magmatism and deformation in the  
78 orogen located at the overriding plate margin of New Zealand have found no conclusive  
79 evidence that shows that subduction must have continued beyond 105-100 Ma (e.g., Bradshaw,  
80 1989; Luyendyk, 1995; Mortimer et al., 2019; Crampton et al., 2019). A 105-100 Ma age  
81 estimate for subduction cessation is commonly inferred from a change in deformation within  
82 New Zealand from largely compression to a regime dominated by extension (e.g., Bradshaw,  
83 1989; Luyendyk, 1995; Crampton et al., 2019), coeval changes in the geochemical signature of  
84 magmatism (Muir et al., 1997; Waight et al., 1998; Tulloch and Kimbrough, 2003; Tulloch et al.,  
85 2009; Van der Meer et al., 2016; 2017; 2018), and angular unconformities in the New Zealand  
86 forearc (Laird and Bradshaw, 2004; Crampton et al., 2019; Gardiner et al., 2021; 2022). On the  
87 other hand, global plate reconstructions suggest that convergence across the Zealandia margin  
88 of New Zealand continued until at least the end of spreading in the Osbourn Trough, of which  
89 estimates vary from ~101 Ma to 79 Ma, based on dredge samples and tentative marine  
90 magnetic anomaly identification (Billen and Stock, 2000; Worthington et al., 2006; Seton et al.,  
91 2012; Zhang and Li, 2016; Mortimer et al., 2019), with widely-used global plate reconstructions

92 (Seton et al., 2012; Matthews et al., 2016; Müller et al., 2019) inferring an 86 Ma age that follows  
93 Worthington et al. (2006). This age, however, is based on interpretations of the New Zealand  
94 geological record that is disputed by many New Zealand geologists. Reconciling the geological  
95 and plate kinematic estimates of the age of subduction cessation therefore requires using  
96 kinematic data from the oceanic and continental domain that are independent from interpreted  
97 ages of subduction cessation to avoid circular reasoning in making reconstruction choices.

98 To do so, we analyse the end of East Gondwana subduction along the Zealandia margin  
99 by reassessing both the plate kinematic and orogenic perspectives. First, we evaluate whether  
100 the age for the end of convergence suggested by global plate models changes by using the latest,  
101 and most detailed published marine magnetic anomaly-based isochrons, and by using the range  
102 of estimates for the arrest of Osbourn Trough spreading based on magnetic anomalies or dredge  
103 samples. Our reconstruction includes the evolution and fragmentation of the Phoenix Plate into  
104 its several daughter plates. We use the recent study of Torsvik et al. (2019) who revisited and  
105 modified absolute Pacific Plate models and updated earlier global plate reconstructions. We  
106 consider relative motions across the East Gondwana continental margin as a function of  
107 absolute plate motion models to evaluate when convergence may have ended, and which  
108 process may have been responsible for this cessation. Furthermore, we review aspects of the  
109 architecture and evolution of the Cretaceous New Zealand orogen, and attempt to reconcile the  
110 timing of the end of subduction with the available geological evidence. We will use our results as  
111 a basis for the reconstruction of the demise of the Phoenix Plate's daughters, which resulted  
112 from their capture by the Pacific Plate after cessation of subduction along the Gondwana margin  
113 and the enigmatic transition to the Pacific-Antarctic spreading ridge.

114

## 115 **2. Plate tectonic setting**

116 The south Pacific Ocean today is underlain by the Pacific, Antarctic, and Nazca plates,  
117 separated by trenches from the South American, Antarctic, and Australian plates (Fig. 1). The  
118 oceanic plates of the Pacific Ocean are separated from each other by mid-ocean ridges: the  
119 Pacific-Antarctic Ridge, the East Pacific Rise between the Pacific and Nazca plates, and the Chile  
120 Ridge between the Antarctic and Nazca plates (Fig. 1). Three microplates are present along the  
121 East Pacific Rise: The Juan Fernandez, Easter, and Galapagos microplates.

122 In the west, the Pacific Plate is currently subducting below the Australian Plate at the  
123 Tonga-Kermadec-Hikurangi subduction zone. To the west of this subduction zone is a series of  
124 Cenozoic back-arc basins (e.g., Lau Basin, South Fiji Basin, Norfolk Basin; e.g., Yan and Kroenke,  
125 1993; Sdrolias et al., 2003; Herzer et al., 2011), bounded in the west by the extended continental  
126 crust of Zealandia that underlies the Lord Howe Rise and Norfolk Ridge (e.g., Mortimer et al.,  
127 2017). Zealandia is separated from the Australian continent by the Upper Cretaceous-Paleogene

128 Tasman Sea and New Caledonia basins (e.g., Gaina et al., 1998; Grobys et al., 2008). The Norfolk  
129 Ridge was overthrust from the east during the Oligocene (c. 30 Ma) by the Paleocene New  
130 Caledonia ophiolite (Cluzel and Meffre, 2002; Cluzel et al., 2012). Ophiolite obduction occurred  
131 during cessation of a northeast-dipping intra-oceanic subduction zone that formed around 60  
132 Ma. At this time other ophiolites also formed that were emplaced during the Late Oligocene onto  
133 Northland, New Zealand, and northward towards the Louisiade Plateau and the eastern Papuan  
134 Peninsula (Fig. 1) (Whattam et al., 2006; Cluzel et al., 2012; Van de Lagemaat et al., 2018a;  
135 Maurizot et al., 2020a; McCarthy et al., 2022).

136 At its northern end, southwest of Samoa, the Tonga-Kermadec-Hikurangi subduction  
137 turns sharply to the west (Fig. 1). Here the plate boundary changes to a SW-trending, diffuse  
138 transform system around the Fiji Islands, southwest of which it continues as the Hunter fracture  
139 zone that connects to the New Hebrides Trench. At this trench the Australian Plate is subducting  
140 below the North Fiji back-arc basin that hosts spreading ridges with the Pacific Plate. The  
141 southern end of the Tonga-Kermadec-Hikurangi subduction zone connects via the right-lateral  
142 Alpine Fault to the Puysegur Trench where subduction of the Australian Plate below the Pacific  
143 Plate is occurring (e.g., Collot et al., 1995; House et al., 2002; Gurnis et al., 2019). The plate  
144 boundary ends at the Macquarie Triple Junction, where the Australian, Pacific, and Antarctic  
145 plates meet, and where the Macquarie microplate formed c. 7 Ma (Cande and Stock, 2004a; Choi  
146 et al., 2017). Kinematic reconstructions of Cenozoic tectonic history of the SW Pacific realm  
147 differ in the timing and distribution of convergence over the New Caledonia and Tonga-  
148 Kermadec subduction zones (Hall, 2002; Schellart et al., 2006; Whattam et al., 2008; Van de  
149 Lagemaat et al., 2018a), but mostly agree on the pre-late Cretaceous position of Zealandia  
150 against the Australian continent, and on the location of the subduction zone along the eastern  
151 Zealandia margin that consumed the Phoenix Plate and its daughters (Fig. 2).

152 The southern boundary of the Pacific Plate is the Pacific-Antarctic Ridge (Fig. 1B). This  
153 plate boundary formed c. 89 Ma, based on the extrapolation of spreading rates from the oldest  
154 identified marine magnetic anomaly (C34y; 83.7 Ma) towards the continental margin (Wobbe et  
155 al., 2012). This age is in correspondence with the  $83.9 \pm 0.1$  Ma age of the Erik seamount,  
156 obtained from Ar/Ar dating of K-feldspar of a trachyte sample, which provides a minimum age  
157 of the oceanic crust (Mortimer et al., 2019). The Pacific-Antarctic Ridge accommodated the  
158 divergence of the Campbell Plateau (part of the Zealandia continent, located on the Pacific Plate)  
159 from Marie Byrd Land (located on the West Antarctic Plate) (e.g., Wobbe et al., 2012). Before  
160 break-up, the Campbell Plateau and West Antarctica formed part of the upper plate adjacent to  
161 the Mesozoic active margin of East Gondwana (Fig. 2) (e.g., Larter et al., 2002). This margin was  
162 contiguous with the active margins of the Antarctic Peninsula and South America, where  
163 subduction remains active today. Presently, subduction of a small remnant of the last of the

164 Phoenix Plate's daughters, the Aluk Plate (Herron and Tucholke, 1976), is ongoing below the  
165 northern part of the Antarctic Peninsula (Fig. 1) (e.g. Eagles, 2004). The Aluk Plate is often also  
166 referred to as Phoenix Plate, but we prefer the name Aluk Plate to make the distinction with the  
167 original parent Phoenix Plate. Subduction below Antarctica progressively ceased with the  
168 arrival of different segments of the Aluk-Antarctica Ridge. A small segment of this ridge remains  
169 in the Southeast Pacific Ocean, which became extinct c. 3.3 Ma (Eagles, 2004), effectively  
170 merging the Aluk Plate with the Antarctic Plate. Subduction below the Antarctic Peninsula is  
171 currently accommodated by opening of the Bransfield Basin within the upper Antarctic Plate  
172 (Fig. 1; Galindo-Zaldívar et al., 2004). The eastern boundary of the Aluk Plate is the Shackleton  
173 Fracture Zone, separating it from the West Scotia Sea. Opening of the Scotia Sea oceanic basins  
174 was not related to plate motions of the paleo-Pacific realm (Van de Lagemaat et al., 2021) and  
175 the Shackleton Fracture Zone is thus the eastern boundary of our reconstruction. To the north  
176 of the Shackleton Fracture Zone, the Antarctic Plate, Chile Ridge, and Nazca Plate are subducting  
177 below South America.

178         Mesozoic subduction of Phoenix Plate lithosphere was accommodated along the  
179 Antarctica and Zealandia margins of East Gondwana (Fig. 2). Breakup of these continents from  
180 each other and from Australia led to oceanic spreading around 84 Ma in both the Tasman Sea  
181 and South Pacific Ocean (Gaina et al., 1998; Wobbe et al., 2012; Mortimer et al., 2019), but  
182 continental rifting between Zealandia and Antarctica and between Zealandia and Australia has  
183 been considered to date back to c. 105-100 Ma (Bradshaw, 1989; Luyendyk, 1995; Laird and  
184 Bradshaw, 2004). Earliest extension between Australia and Antarctica started at c. 136 Ma  
185 (Whittaker et al., 2013).

186         A prominent record of Mesozoic subduction is present in New Zealand. The Eastern  
187 Province consists of Permian intra-oceanic arc sequences and a long-lived Mesozoic  
188 accretionary wedge (Fig. 3) (Mortimer, 2004; Mortimer et al., 2014). It is possible that the  
189 Eastern Province hosts the records of two subduction systems, one along the Gondwana margin  
190 and one intra-oceanic (Adams et al., 2007; Van de Lagemaat et al., 2018b; Campbell et al., 2020),  
191 but these have been juxtaposed since at least the latest Jurassic (Tulloch et al., 1999), i.e.,  
192 throughout the window of interest of this paper. The western and eastern provinces are  
193 separated by the Median Batholith that represents a long-lived Paleozoic to Mesozoic magmatic  
194 arc (Fig. 2 and 3) (Mortimer, 2004). The accretionary wedge of the Eastern Province consists of  
195 ocean plate stratigraphy (OPS; Isozaki et al., 1990) comprising pillow lavas, oceanic pelagic and  
196 hemipelagic sediments, and trench fill clastics (Caples, Waipapa and Torlesse terranes;  
197 Mortimer et al., 2014). These OPS sequences accreted to the Gondwana margin from Permian to  
198 Early Cretaceous times and were intruded by magmatic arc plutons and overlain by forearc  
199 basin clastics (Adams et al., 1998; Mortimer, 2004; Boschman et al., 2021a). The geology of New

200 Caledonia shares broad similarities with that of New Zealand: The Boghen Terrane of New  
201 Caledonia has been correlated to the Torlesse Complex of New Zealand; both Jurassic-  
202 Cretaceous accretionary complexes, and the Teremba Terrane of New Caledonia to the Murihiku  
203 Terrane of New Zealand; both forearc terranes consisting of late Permian to Jurassic island-arc  
204 derived strata (Cluzel and Meffre, 2002; Maurizot et al., 2020b). Cretaceous sedimentary  
205 sequences that overlie the Torlesse accretionary complex from 100 Ma onwards in New Zealand  
206 (Laird and Bradshaw, 2004; Crampton et al., 2019) provide important arguments for  
207 interpreting the end of subduction: they are widely seen as signaling a transition from a  
208 subduction margin to a passive margin (e.g., Field and Uruski, 1997; Laird and Bradshaw, 2004;  
209 Edbrooke, 2017; Crampton et al., 1999; 2019). However, others have considered these Late  
210 Cretaceous sequences to be accretionary shelf and slope basin fill that accumulated during  
211 outbuilding of the accretionary wedge and that subduction continued until c. 84 Ma (Mazengarb  
212 and Harris, 1994; Kamp, 1999; 2000; Gardiner and Hall, 2021). Deposition of subduction-  
213 related volcanoclastic greywackes continued until c. 90 Ma in New Caledonia (Cluzel et al., 2010;  
214 Maurizot et al., 2020b)

215         The oceanic lithosphere of the modern Pacific Plate contains three prominent oceanic  
216 plateaus interpreted to have formed as a single ~120 Ma Large Igneous Province (LIP): the  
217 conceptual Ontong Java Nui LIP (Taylor, 2006; Chandler et al., 2012). The three oceanic plateaus  
218 that are thought to have once formed as Ontong Java Nui are currently separated by post-120  
219 Ma Cretaceous oceanic basins. These oceanic plateaus are the Ontong Java Plateau, located to  
220 the north of the Solomon Islands; the Manihiki Plateau, located to the northeast of Samoa; and  
221 the Hikurangi Plateau, located offshore the North Island of New Zealand (Fig. 1). The Manihiki  
222 Plateau is separated from the Ontong Java Plateau by the Ellice Basin, and the Hikurangi Plateau  
223 is separated from the Manihiki Plateau by the Osbourn Trough (Fig. 1).

224

### 225 **3. Reconstruction approach, plate circuits, and reference frames**

226         Quantitative constraints on the convergence history between the plates of the  
227 Panthalassa realm and the Zealandia margin of East Gondwana follows from the kinematic  
228 reconstruction of the South Pacific region. The reconstruction presented here includes a  
229 compilation of the most recent kinematic data and the new Pacific reference frame of Torsvik et  
230 al. (2019). For the analysis in this paper, we focus on the history of the South Pacific region back  
231 to the Early Cretaceous. Our reconstruction is made in GPLates, a freely available plate  
232 reconstruction software ([www.gplates.org](http://www.gplates.org); Boyden et al., 2011; Müller et al., 2018).

233         We restore spreading along the different mid-ocean ridges that existed in the southern  
234 Panthalassa realm based on published marine magnetic anomaly data of ocean floor presently  
235 underlying the south Pacific Ocean (Fig. 4), reviewed in section 4. The ages of the polarity

236 chrons in our reconstruction are updated to the timescale of Ogg (2020). We incorporate all  
237 rotation poles as published, even though on short time intervals (<1 Myr) these are likely  
238 subject to some noise (Iaffaldano et al., 2012). Our conclusions, however, are not affected by the  
239 short time-scale noise and we prefer to see the effect of all interpreted isochrons rather than an  
240 arbitrary selection of these.

241 In the absence of polarity reversals during the Cretaceous Normal Superchron (121.4-  
242 83.7 Ma), the restoration of oceanic basins for this time interval is based on previously  
243 published radiometric data from dredged and cored samples as well as published  
244 interpretations of seafloor fabric (Fig. 4; see section 4). Magnetic anomaly picks and fracture  
245 zone data were obtained from the GSFML Database (Seton et al., 2014). We restore intra-  
246 continental deformation within East Gondwana applying a reconstruction hierarchy that uses  
247 quantitative kinematic constraints on continental extension, transform motion, or crustal  
248 shortening (see Boschman et al., 2014 and Van de Lagemaat et al., 2018a for details).

249 Plate convergence can best be quantified when a plate circuit is present that connects  
250 the two converging plates through a series of active or fossil spreading ridges (Cox and Hart  
251 1986). For times after the formation of the Pacific-Antarctic Ridge (Chron C34y, c. 83.7 Ma; see  
252 section 4), plate convergence in the region can be reconstructed through a plate circuit that  
253 constrains the motion of the Australian Plate relative to the Antarctic Plate based on the record  
254 of oceanic spreading at the Southeast Indian Ridge (SEIR), and the motion of the Pacific Plate  
255 relative to the Antarctic Plate by restoring spreading at the Pacific-Antarctic Ridge (PAR) (Fig.  
256 5). The Late Cretaceous and Cenozoic opening of marginal and back-arc basins east of Australia  
257 are reconstructed relative to the Australian Plate, that adds Zealandia-Australia, and Tonga-  
258 Kermadec-Hikurangi trench-Zealandia motion to the plate circuit. In addition, the relative  
259 motion of oceanic plates flooring the Pacific Ocean are reconstructed relative to the Pacific Plate  
260 (Fig. 5). For the period of activity of the New Caledonia subduction zone in Paleocene to  
261 Oligocene time, it is not possible to quantify partitioning of convergence over the Tonga and  
262 New Caledonia trenches – only net convergence between Zealandia and the Panthalassa plates  
263 can be quantified (Van de Lagemaat et al., 2018a). However, for the interval of interest of this  
264 paper, this problem is of no consequence.

265 For times after the Cretaceous Normal Superchron, i.e. at C34y (post-83.7 Ma), we use  
266 the ‘Antarctic’ plate circuit Zealandia – Australia – East Antarctica – West Antarctica – Pacific  
267 (Fig. 5). Due to uncertainties in relative motion between West Antarctica and East Antarctica  
268 before 45 Ma, some studies use a plate circuit for these times that ties the Lord Howe Rise to the  
269 Pacific Plate directly before c. 45 Ma instead (i.e., the Australian circuit) using magnetic  
270 anomalies in the Tasman Sea basin (e.g., Steinberger et al., 2004; Torsvik et al., 2019). In the  
271 Australian circuit it is assumed that there is no plate boundary between the Pacific Plate and



272 Zealandia between 83 and 45 Ma. However, geological data from New Caledonia provides  
273 evidence for the existence of a subduction zone between the Pacific Plate and the Norfolk Ridge  
274 between c. 60 and 30 Ma (e.g. Cluzel et al., 2012; Van de Lagemaat et al., 2018a; Maurizot et al.,  
275 2020b), which means that the Pacific Plate should not be reconstructed relative to Zealandia  
276 after 60 Ma. Combined with recently improved constraints on deformation within Antarctica  
277 (e.g. Granot et al., 2013; Granot and Dymant, 2018) leads us to prefer the Antarctic circuit for  
278 our reconstruction, similar to Seton et al. (2012), Matthews et al. (2015), and Müller et al.  
279 (2019). There is a c. 150 km difference in location of the Pacific relative to the Gondwana plates  
280 between the Antarctic and Australian circuits at chron C34y (83.7 Ma).

281 Before the onset of Pacific-Antarctic Ridge spreading, the plate circuit is broken, as the  
282 Panthalassa and Gondwana plates are connected through a subduction zone only (Seton et al.,  
283 2012; Wright et al., 2016). The reconstruction of pre-chron C34y (83.7 Ma) relative motions  
284 across the East Gondwana margin then relies on placing the Gondwana continents and the  
285 Panthalassa plates in mantle reference frames that were developed for each of the two systems  
286 separately (Fig. 5). For the Panthalassa domain, we use Torsvik et al. (2019), who updated a  
287 fixed hotspot frame that constrains absolute Pacific Plate motion back to 150 Ma and showed  
288 that previous Pacific reference frames are flawed. The Gondwana continents are part of the  
289 Indo-Atlantic realm, whose relative motions are constrained by the reconstruction of the Indian  
290 and Atlantic Oceans. Several mantle reference frames are available for the Indo-Atlantic realm,  
291 from different approaches and iterations. We will illustrate the sensitivity of the choice of  
292 reference frame for convergence across the Zealandia margin, using the moving hotspot  
293 reference frames of O'Neill et al. (2005), Torsvik et al. (2008), and Doubrovine et al. (2012), and  
294 the semi-quantitative slab-fitted reference frame of Van der Meer et al. (2010). These reference  
295 frames are given in African coordinates, requiring reconstructing the eastern Gondwana  
296 continents circuit to the African Plate.

297

#### 298 **4. Review of kinematic data**

##### 299 **4.1. Post-Cretaceous Quiet Zone plate reconstruction of ocean basins, and East** 300 **Gondwana fit**

301 The onset of spreading at the Pacific-Antarctic Ridge marks a major break in the plate  
302 tectonic history of the Panthalassa-Pacific realm, as it formed the first passive margin that  
303 connected the oceanic domain to the Indo-Atlantic plates after hundreds of millions of years  
304 (e.g., Seton et al., 2012; Wright et al., 2016 Müller et al., 2019). The oldest magnetic anomaly that  
305 records spreading between the Campbell Plateau and Marie Byrd Land (West Antarctica) is  
306 chron C33 (79.9 Ma; Wobbe et al., 2012), the oldest crust having formed after the end of chron  
307 C34y, i.e., after 83.7 Ma. Farther east, however, the marine magnetic anomaly of chron C34y

308 (83.7 Ma) was identified just south of Chatham Rise and its conjugate margin off the coast of  
309 Thurston Island (Larter et al., 2002; Eagles et al., 2004a; Wobbe et al., 2012). There is no  
310 evidence for the existence of a plate boundary between the oceanic crust that formed south of  
311 the Chatham Rise and the Campbell Plateau and oceanic crust of the Pacific Plate, and it is  
312 therefore assumed that the Chatham Rise and Campbell Plateau have been part of the Pacific  
313 Plate since the formation of the Pacific-Antarctic Ridge (Molnar et al., 1975; Luyendyk, 1995).  
314 The set of marine magnetic anomalies of chron C34y (83.7 Ma) that formed south of Chatham  
315 Rise and off the coast of Thurston Island is therefore the oldest marine magnetic anomaly  
316 constraint for Pacific-West Antarctica spreading (Wobbe et al., 2012; Wright et al., 2016). As  
317 these marine magnetic anomalies are located close to the continental margins of Chatham Rise  
318 and West Antarctica, it is thought that true seafloor spreading started shortly before the end of  
319 the Cretaceous Quiet Zone (Wobbe et al., 2012). Based on the extrapolation of seafloor  
320 spreading rates, Wobbe et al. (2012) suggested that the first oceanic crust between Chatham  
321 Rise and Thurston Island (West Antarctica) formed around 84 Ma, which is in accord with the  
322 minimum age for the oceanic crust between Chatham Rise and West Antarctica, based on a  $83.9$   
323  $\pm 0.1$  Ma Ar/Ar age of K-feldspar in a trachyte sample from Erik Seamount (Mortimer et al.,  
324 2019), while rifting is thought to have started around 89 Ma (Wobbe et al., 2012). The oldest  
325 oceanic crust between Chatham Rise and West Antarctica may have formed during extension in  
326 the Bounty Trough (between 92 and 84 Ma; Grobys et al., 2008), before Chatham Rise was  
327 captured by the Pacific Plate. The timing of the capture of Chatham Rise by the Pacific remains  
328 uncertain, although it must have occurred in the 90-83.7 Ma interval: the location of the Pacific  
329 Plate is constrained at either end of this time interval: 90 Ma is the youngest age in the Pacific  
330 hotspot reference frame of Torsvik et al. (2019) and 83.7 Ma (i.e., chron C34y) is the oldest  
331 marine magnetic anomaly constraint (Wright et al., 2016). Between those times (90-83.7 Ma),  
332 the Pacific Plate may have started to diverge from West Antarctica, but we reconstruct the start  
333 of Pacific-Antarctic spreading based on the oldest marine magnetic anomaly constraint (i.e.,  
334 C34y; 83.7 Ma; Wobbe et al., 2012), similar to other reconstructions (e.g., Seton et al., 2012;  
335 Wright et al., 2016; Müller et al., 2019). Any extension in the region (i.e., between Chatham Rise  
336 and Campbell Plateau and West Antarctica) before that time is considered to not have involved  
337 the Pacific Plate (Fig. 6D and Fig. 7C). We reconstruct the motion between the Pacific Plate and  
338 West Antarctica using finite rotation poles of Croon et al. (2008) (present-C20; 43.5 Ma) and  
339 Wright et al. (2016) (C21-C34y; 47.8-83.7 Ma). This is similar to the reconstruction of Müller et  
340 al. (2019), although we incorporate all published rotation poles whereas Müller et al. (2019)  
341 only used rotation poles for selected polarity chrons.

342         Shortly before the start of chron C33 (79.9 Ma) a piece of lithosphere broke off of West  
343 Antarctica to form the Bellingshausen Plate (Stock and Molnar, 1987). The Bellingshausen Plate

344 started to rotate clockwise relative to West Antarctica and acted as an independent plate until  
345 chron C27 (62.5 Ma; Stock and Molnar, 1987; Cande et al., 1995; Eagles et al., 2004b; Wobbe et  
346 al., 2012; Wright et al., 2016). During this time window, the northern margin of the  
347 Bellingshausen Plate was formed by a spreading ridge with the Pacific Plate and its western  
348 margin was defined by a short transform margin with the Marie Byrd Land sector of West  
349 Antarctica, close to the Euler pole of Bellingshausen-West Antarctica motion (Wright et al.,  
350 2016). To the east, the Bellingshausen Plate was bounded by a right-lateral transform fault from  
351 the Aluk Plate (Larter et al., 2002; Eagles et al., 2004). To the south, the Bellingshausen Plate  
352 was converging with the Thurston Island sector of West Antarctica, although the maximum total  
353 amount of convergence was less than 250 km and no mature subduction zone developed  
354 (Wright et al., 2016). Like the reconstruction of Müller et al. (2019), we reconstruct the 79.9-  
355 62.5 Ma motion of the Bellingshausen Plate relative to the Pacific Plate using the finite rotation  
356 poles of Wright et al. (2016), which are based on marine magnetic anomalies of chrons C33-C27.

357 We tentatively suggest that friction at the transform fault that formed the eastern plate  
358 boundary of the West Antarctic Plate (Heezen Fracture Zone) led to the partial coupling of West  
359 Antarctica with the Aluk Plate. After the formation of the Pacific-Antarctic ridge, the Pacific-  
360 West Antarctica spreading and Pacific-Aluk spreading ridges were parallel, but Pacific-Aluk  
361 spreading occurred at a higher rate (~3.5 and ~7 cm/yr half-spreading rate, respectively). This  
362 resulted in lengthening of the transform fault that formed the plate boundary between the West  
363 Antarctic and Aluk plates. The partial coupling of part of West Antarctica with Aluk caused the  
364 formation of the Bellingshausen Plate, which was being dragged along by the Aluk Plate. This  
365 dragging resulted in clockwise rotation of Bellingshausen relative to West Antarctica. This  
366 suggestion is similar to what was proposed by Eagles et al. (2004b), who also suggested that the  
367 independent motion of Bellingshausen was related to the lengthening of the West Antarctica-  
368 Pacific transform plate boundary. A similar process was responsible for the formation of e.g. the  
369 Bauer microplate, which moved independently between c. 18-6 Ma, partitioning strain between  
370 the Pacific and Nazca plates (Eakins and Lonsdale, 2003).

371 Before C34y (83.7 Ma), pre-drift extension had already started to separate the Campbell  
372 Plateau from Marie Byrd Land and Chatham Rise from the Campbell Plateau (Molnar et al.,  
373 1975; Stock and Cande, 2002; Riefstahl et al., 2020) (Fig. 6D and 7C). We reconstruct c. 180 km  
374 of pre-drift extension between the Campbell Plateau and Marie Byrd Land between 95 and 83.7  
375 Ma, based on the estimated 90 km of extension in both margins based on crustal thickness  
376 calculations (Wobbe et al., 2012). We reconstruct c. 200 km of extension in the Bounty Trough  
377 (between Chatham Rise and the Campbell Plateau) between 92 and 84 Ma, based on the  
378 reconstruction derived from crustal thickness calculations of Grobys et al. (2008). This  
379 reconstruction also leads to extension between Chatham Rise and the Thurston Island sector of

380 West Antarctica, where plate boundary activity may have started around 89 Ma (Wobbe et al.,  
381 2012).

382 A long-lived volcanic arc and accretionary prism on the Antarctic Peninsula shows that  
383 subduction continued throughout the Mesozoic and Cenozoic until the present-day (e.g., Burton-  
384 Johnson and Riley, 2015; Jordan et al., 2020). The plate that is subducting below the Antarctic  
385 Peninsula, the Aluk Plate, is therefore thought to be a descendent of the Phoenix Plate (Fig. 1;  
386 e.g., Barker, 1982; Eagles, 2004). Interestingly, however, for much of the Cenozoic, and until the  
387 cessation of spreading around 3.3 Ma, the Aluk Plate has not been spreading relative to the  
388 Pacific Plate, but relative to oceanic lithosphere of West Antarctica (Eagles, 2004). Marine  
389 magnetic anomalies that formed along the Aluk-West Antarctica Ridge are preserved on the  
390 Aluk Plate back to C6A (21.32 Ma; Larter and Barker, 1991; Eagles, 2004), and on conjugate  
391 West Antarctica oceanic lithosphere back to C27 (62.52 Ma) (Cande et al., 1982). To the  
392 northwest, West Antarctica also contains a set of magnetic anomalies from C21 (47.8 Ma) and  
393 younger that record spreading between West Antarctica and the Pacific Plate (Cande et al.,  
394 1982; Cande et al., 1995; Croon et al., 2008). This spreading was near-parallel to West  
395 Antarctica-Aluk spreading, showing simultaneous and near-parallel spreading of West  
396 Antarctica with both the Pacific and Aluk plates (Wright et al., 2016).

397 Around the time of chron C21 (c. 47 Ma), part of the Pacific Plate that formed through  
398 Pacific-Aluk spreading was captured by the West Antarctic Plate (Cande et al., 1982; McCarron  
399 and Larter, 1998; Eagles et al., 2004a). Shortly before capture, the transform plate boundary  
400 between the West Antarctic and Pacific plates was lengthening due to the higher Pacific-Aluk  
401 compared to Pacific-West Antarctic spreading rates, similar to the situation that resulted in the  
402 formation of the Bellingshausen Plate. During capture, the Pacific-Antarctic ridge propagated  
403 into oceanic crust of the Pacific Plate that formed around C27 (c. 62.5 Ma) (Cande et al., 1982).  
404 At the southern end of the captured crust, the Pacific-Aluk ridge was replaced by the West  
405 Antarctic-Aluk ridge.

406 To the northeast, West Antarctica shared a spreading ridge with the Farallon Plate and  
407 its daughter Nazca Plate (Fig. 6H-J) (Wright et al., 2016). However, before C21 (47.3 Ma), there  
408 was no Antarctic oceanic crust that separated the Aluk Plate from the Pacific Plate (Fig. 6G):  
409 instead, the Aluk Plate was spreading directly with the Pacific Plate, recorded by marine  
410 magnetic anomalies back to C34y (83.7 Ma) on the Pacific Plate (Cande et al., 1982; Cande et al.,  
411 1995; Larter et al., 2002; Eagles et al., 2004a; Croon et al., 2008). In our reconstruction we use  
412 rotation poles of Aluk-West Antarctica and Aluk-Pacific motion back to C34y (83.7 Ma) of Eagles  
413 (2004), Eagles and Scott (2014) and Wright et al. (2016), similar to Müller et al. (2019). The  
414 tectonic history of the Aluk Plate prior to C34y (83.7 Ma) cannot be constrained by magnetic  
415 anomalies due to the Cretaceous Quiet Zone.

416           In the East Pacific, the Nazca Plate is spreading along the East Pacific Rise from the  
417 Pacific Plate and along the Chile Ridge from West Antarctica, while subducting below South  
418 America (Fig. 1). The Nazca Plate formed c. 22 Ma (chron C6B), as the southern remnant of the  
419 broken up Farallon Plate (Barckhausen et al., 2001; 2008; Wright et al., 2016). The East Pacific  
420 Rise records spreading between the Pacific and Nazca plates (and its predecessor the Farallon  
421 Plate) back to chron C23 (51.7 Ma) on the Nazca Plate (older magnetic anomalies have been lost  
422 to subduction below South America) and back to chron C34y (83.7 Ma) on the Pacific Plate  
423 (Atwater and Severinghaus, 1989; Barckhausen et al., 2008; Wilder, 2003; Handschumacher et  
424 al., 1976). Spreading between the Nazca Plate and West Antarctica is recorded at the Chile Ridge  
425 back to chron C24 (53.9 Ma) on West Antarctica and back to chron C5E (18.5 Ma) on the Nazca  
426 Plate (Cande et al., 1982; Tebbens et al., 1997). We reconstruct the Nazca Plate relative to the  
427 Pacific Plate, using the finite rotation poles based on marine magnetic anomalies back to chron  
428 C6B (22.3 Ma) of Tebbens and Cande (1997), as published in Wright et al. (2016), similar to  
429 Müller et al. (2019). We include the Bauer Microplate that formed in Miocene times at the  
430 Nazca-Pacific ridge using magnetic anomalies C5E-C3A (18.5-6.7 Ma) identified by Eakins and  
431 Lonsdale (2003), with rotations computed in GPlates. We do not include the Galapagos, Easter  
432 and Juan Fernandez microplates in our reconstruction, which formed about 5 Ma (Tebbens and  
433 Cande, 1997; Wright et al., 2016). The Farallon Plate is reconstructed relative to the Pacific Plate  
434 between 22.3 (chron C6B) and 83.7 Ma (chron C34y) using the finite rotations poles of Wright  
435 et al. (2016), like in Müller et al. (2019). The record of Farallon-Pacific spreading during and  
436 before the Cretaceous Quiet Zone will be discussed in section 4.2.

437           Cenozoic relative motion between East Antarctica and West Antarctica is constrained by  
438 marine magnetic anomalies that formed in the Adare and Northern basins between chrons C5  
439 and C27 (11.1-62.5 Ma) (Cande and Stock, 2004; Granot et al., 2013; Granot and Dymant, 2018).  
440 We incorporate the finite rotation poles of Granot and Dymant (2018), Granot et al. (2013), and  
441 Cande and Stock (2004) for chrons C5-C8, C12-C18, and C20-C27, respectively. Mesozoic  
442 extension in the West Antarctic Rift System (WARS) between West Antarctica and East  
443 Antarctica is poorly constrained, but a main phase of extension was proposed to have occurred  
444 in the mid-Late Cretaceous, based on low temperature geochronology studies (Lawver and  
445 Gahagan, 1994; Fitzgerald, 2002; Spiegel et al., 2016; Veevers, 2012). Based on crustal thickness  
446 estimates (An et al., 2015; Llubes et al., 2018; Shen et al., 2018), we reconstruct c. 100 km of  
447 extension in the West Antarctic Rift System between 95 and 84 Ma (Fig. 7).

448           Australia-East Antarctica motion is based on marine magnetic anomalies back to chron  
449 C34y (83.7 Ma), although seafloor spreading was slow before chron C17o (~38 Ma) (Cande and  
450 Stock, 2004b; Whittaker et al., 2007; 2013). Pre-drift extension between East Antarctica and  
451 Australia started at 136 Ma (Whittaker et al., 2013), and we base the East Gondwana fit of East

452 Antarctica and Australia on the reconstruction of the extended conjugate continental margins of  
453 Williams et al. (2011) and Gibbons et al. (2012). Our Australia-East Antarctica reconstruction is  
454 similar to that of Müller et al. (2019).

455 The Late Cretaceous to early Eocene separation of Lord Howe Rise (North Zealandia)  
456 from Australia is recorded by marine magnetic anomalies C24-C34y (53.9-83.7 Ma) in the  
457 Tasman Sea (Gaina et al., 1998). We use the finite rotation poles of Gaina et al. (1998) in our  
458 reconstruction, like Seton et al. (2012) and Müller et al. (2019). Pre-drift extension is thought to  
459 have started c. 95 Ma, concurrently with extension in the New Caledonia Basin, between the  
460 Norfolk Ridge and Lord Howe Rise (Fig. 6D-E and 7C) (Groby et al., 2008). The back-arc basins  
461 between Lord How Rise and the Tonga-Kermadec-Hikurangi subduction zone are reconstructed  
462 as in Van de Lagemaat et al. (2018a), using marine magnetic anomaly constraints from Yan and  
463 Kroenke (1993), Sdrolias et al. (2003), and Herzer et al. (2011).

464 We connect the plate circuit of our reconstruction to Africa by reconstructing East  
465 Antarctica-Africa motion through the South Atlantic Ocean. This is based on finite rotation poles  
466 based on marine magnetic anomalies back to chron M38 (c. 164 Ma) of DeMets et al. (2021) (C1-  
467 C23; 0-51.7 Ma), Cande et al. (2010) (C23-C29; 51.7-64.9 Ma), Bernard et al. (2005) (C29-C33;  
468 64.9-79.9 Ma), and Mueller and Jokat (2019) (C34y-M38; 84.7-162.9 Ma).

469

## 470 **4.2. Pre-C34y plate reconstruction of the Paleo-Pacific realm**

### 471 **4.2.1. Evolution of the Phoenix Plate**

472 Direct kinematic constraints on the evolution of the Phoenix Plate come from marine  
473 magnetic anomalies preserved on the Pacific Plate (Nakanishi et al., 1992). The oldest of these  
474 anomalies, preserved in the west Pacific Ocean, formed at the Pacific-Phoenix Ridge (Larson and  
475 Chase, 1972), and were identified as M29n.2n – M1n (Nakanishi et al., 1992), indicating that  
476 Pacific-Phoenix spreading was active from at least 155.9 to 123.8 Ma. We reconstruct the  
477 motion of Phoenix for this time interval using GPlates, by mirroring the marine magnetic  
478 anomalies that are preserved on the Pacific Plate, assuming symmetric spreading (Fig. 6A-B).  
479 We reconstruct Pacific-Phoenix spreading until 120 Ma, the timing of Ontong Java Nui break-up  
480 (see section 4.2.2) (Taylor, 2006; Chandler et al., 2012).

481 While Pacific-Phoenix spreading was active, the Pacific Plate was also spreading with the  
482 Farallon and Izanagi plates (or Izanami Plate; see Boschman et al., 2021b). Marine magnetic  
483 anomalies that formed during chrons M29 – M0 (156.9-121.4 Ma) were identified on the  
484 eastern side of the Pacific triangle (Nakanishi et al., 1992), which constrain spreading between  
485 the Pacific and Farallon plates. Pacific-Izanagi spreading is constrained by marine magnetic  
486 anomalies that formed during chrons M35 – M5 (160.9-127.5 Ma) (Nakanishi et al., 1992). We  
487 reconstruct Farallon-Pacific and Izanagi-Pacific spreading in this time interval based on the

488 marine magnetic anomalies (Nakanishi et al., 1992), using the reconstruction poles of Boschman  
489 et al. (2021a).

490 Marine magnetic anomalies that formed in the southeast corner of the Pacific triangle  
491 suggest the formation of two microplates (the Trinidad and Magellan microplates) around the  
492 Pacific-Farallon-Phoenix triple junction (Nakanishi and Winterer, 1998). The Trinidad  
493 microplate formed around chron M21 (146.6 Ma) and stopped acting as a separate plate around  
494 chron M14 (136.9 Ma) (Nakanishi and Winterer, 1998). The Magellan microplate formed  
495 around chron M15 (138.5 Ma) and remained active until chron M9 (129.9 Ma), when it merged  
496 with the Pacific Plate (Nakanishi and Winterer, 1998). We incorporate the independent motion  
497 of the Magellan microplate between chrons M15 and M9 (138.5 – 129.9 Ma) in the  
498 reconstruction. We computed finite rotation poles for this reconstruction in GPlates, based on  
499 the magnetic anomaly picks of Nakanishi and Winterer (1998). We do not reconstruct the  
500 Trinidad microplate, because there are not enough marine magnetic anomaly identifications for  
501 a reliable reconstruction of this microplate.

502 From reconstruction of Pacific-Farallon and Pacific-Izanagi spreading, it follows that the  
503 Phoenix Plate also formed mid-oceanic ridges with the Farallon and Izanagi plates (Fig. 6A). The  
504 location of these spreading ridges relative to the Pacific triangle is unknown, but undated  
505 marine magnetic anomalies in the Caribbean plate have orientations that are consistent in  
506 direction with those that would have formed at the Farallon-Phoenix ridge, and ages of ocean  
507 floor exposed in western Costa Rica are consistent with a Jurassic age of spreading of this  
508 lithosphere (Boschman et al., 2019). This suggests that prior to the Cretaceous Quiet Zone, the  
509 Farallon-Phoenix ridge was located at the longitude of (and subducting below) northern South  
510 America. The Izanagi-Phoenix ridge is generally assumed to have remained north of Australia  
511 (e.g. Seton et al., 2012). The Phoenix Plate and its Cretaceous to Cenozoic daughters were  
512 therefore lost along a continuous subduction margin that spanned from the Caribbean region,  
513 down along the westcoast of South America, continuing along the West Antarctic and Zealandia  
514 margins to northeast Australia and possibly into Southeast Asia (Fig. 2 and 6A).

515

#### 516 **4.2.2. Ontong Java Nui break-up**

517 The Phoenix lineations on the Pacific Plate are overlain in the west by the Ontong Java  
518 Plateau (Larson, 1997). South of the Phoenix lineations is the oceanic Ellice Basin, which is  
519 devoid of marine magnetic anomalies due to its formation during the Cretaceous Normal  
520 Superchron, but has east-west trending fracture zones (Benyshek et al., 2019). According to the  
521 'superplateau' hypothesis, the Ontong Java Plateau, together with the Manihiki and Hikurangi  
522 plateaus was emplaced as a single Large Igneous Province, known as Ontong Java Nui, around  
523 125-120 Ma (Fig. 6B; Taylor, 2006; Chandler et al., 2012). Shortly after emplacement, Ontong

524 Java Nui broke up into the three modern plateaus through spreading in the Ellice Basin and  
525 Osbourn Trough (Taylor, 2006; Chandler et al., 2012; Hochmuth et al., 2015). The Ontong Java  
526 Nui LIP erupted on either side of the already existing Pacific-Phoenix spreading ridge: the  
527 Ontong Java Plateau represents the part of the LIP that formed on the Pacific Plate, whereas the  
528 Manihiki and Hikurangi plateaus formed on the former Phoenix Plate (Larson, 1997; Seton et al.,  
529 2012). After separation, the Manihiki and Hikurangi plateaus became part of independent  
530 tectonic plates, which grew larger than the original LIPs through the formation of new oceanic  
531 crust at their bounding mid-ocean ridges (Fig. 6B-C) (Seton et al., 2012). We refer to these  
532 plates as the Manihiki and Hikurangi plates. When we discuss the actual LIPs, we will refer to  
533 them as Manihiki and Hikurangi plateaus. Restoration of spreading in the Ellice Basin and  
534 Osbourn Trough reconstructs the Hikurangi Plate via the Manihiki Plate relative to the Pacific.  
535 The emplacement and subsequent break-up of Ontong Java Nui also resulted in the  
536 fragmentation of the Phoenix Plate (e.g. Seton et al., 2012). The spreading history of the Ellice  
537 Basin and Osbourn Trough is thus of key importance in the search of the Phoenix Plate and for  
538 reconstructing the convergence history between the Pacific realm plates and the Zealandia  
539 margin of East Gondwana.

540         The Ontong Java Nui fit of the three plateaus is based on the interpretation of conjugate  
541 rifted margins (Taylor, 2006; Chandler et al., 2012). The general absence of marine magnetic  
542 anomalies in the Cretaceous Quiet Zone makes the opening history of these basins challenging  
543 to reconstruct in detail. The start of opening of the basins postdated the main formation phase  
544 of Ontong Java Nui, which occurred at 125 – 120 Ma. This age is based on  $^{40}\text{Ar}/^{39}\text{Ar}$  dating of  
545 tholeiitic basalts dredged from the three plateaus (Mahoney et al., 1993; Hoernle et al., 2010;  
546 Timm et al., 2011) and on the age of sediments directly overlying pillow basalts (Winterer et al.,  
547 1974; Sliter et al., 1992). Spreading at the Osbourn Trough started before 115 Ma, based on  $115$   
548  $\pm 1$  Ma U-Pb zircon ages from dredged lavas and volcanoclastic sandstones from the West  
549 Wishbone Ridge (Mortimer et al., 2006). Dating of rift-related structures revealed a c. 120 Ma  
550 age of separation between the Hikurangi and Manihiki plateaus (Davy et al., 2008). The onset of  
551 rifting in the Ellice Basin between the Manihiki and Ontong Java plateaus is thought to have  
552 occurred concurrently with the onset of spreading at the Osbourn Trough, although this is not  
553 confirmed by radiometrically dated dredge samples (e.g., Chandler et al., 2012; Hochmuth et al.,  
554 2015).

555         A tectonic reconstruction for the final stages of opening of the Ellice Basin was  
556 presented by Benyshek et al. (2019), based on detailed bathymetric data from the center of the  
557 basin. They tentatively suggested ages for their rotation poles, based on estimated spreading  
558 rates, but these await confirmation by radiometric dating of basement samples (Benyshek et al.,



559 2019). The end of spreading in the Ellice Basin most likely occurred before the end of the CNS,  
560 i.e., before 83.7 Ma.

561         Because no marine magnetic anomalies have been confidently identified, spreading at  
562 the Osbourn Trough is also widely interpreted to have occurred entirely during the Cretaceous  
563 Normal Superchron (e.g., Chandler et al., 2012). The age of arrest of the Osbourn Trough  
564 opening is important for the age of cessation of subduction at the Gondwana margin of New  
565 Zealand. The age of 86 Ma incorporated in the widely used global plate models (Seton et al.,  
566 2012; Matthews et al., 2016; Muller et al., 2019) came from Worthington et al. (2006), who  
567 interpreted the age of arrest of spreading from an age for arrest of subduction based on  
568 geological interpretations from New Zealand: occurrence of calc-alkaline volcanism until 89 Ma  
569 (Smith and Cole, 1997), the interpreted ongoing outbuilding of an accretionary wedge  
570 (Mazengarb and Harris, 1994; Kamp, 1999; 2000) and an 86 Ma episode of metamorphism (Vry  
571 et al., 2004), all recognized in New Zealand. But because this young age of subduction arrest is  
572 widely disputed by the geological community of New Zealand who prefer a 105-100 Ma (e.g.,  
573 Bradshaw, 1989; Luyendyk, 1995; Crampton et al., 2019; Mortimer et al., 2019; Gardiner et al.,  
574 2021), and it is this debate that we aim to reconcile, our reconstruction of Osbourn Trough  
575 should remain independent from the interpretations of the geology of New Zealand. Billen and  
576 Stock (2000) tentatively identified anomalies C33 and C32 (79.9 and 73.6 Ma) in the Osbourn  
577 Trough. Because the magnetic anomalies are not obvious lineations, they called for more  
578 magnetic data and dredge samples. The magnetic anomalies have thus far not been  
579 independently confirmed, but Mortimer et al. (2019) reported an  $84.4 \pm 3.5$  Ma  $^{40}\text{Ar}/^{39}\text{Ar}$  age of  
580 plagioclase in a basalt flow recovered from bore hole DSDP595, which is located c. 200 km north  
581 of the former Osbourn Trough spreading center (Fig. 4). Through extrapolation of spreading  
582 rates, they proposed that Osbourn Trough spreading may have continued until  $\sim 79$  Ma  
583 (Mortimer et al., 2019), implying that spreading may indeed have continued after the  
584 Cretaceous Quiet Zone as suggested by Billen and Stock (2000). However, the 84.4 Ma age is a  
585 tentative age, as the effects of seawater alteration could not be entirely ruled out (Mortimer et  
586 al., 2019). On the other hand, Zhang and Li (2016) suggested that spreading at the Osbourn  
587 Trough ceased around 101 Ma, which would require ultrafast spreading rates of 19 cm/yr. This  
588 is based on a  $103.7 \pm 2.3$  Ma Re-Os isochron age of basalts recovered from bore hole U1365 (Fig.  
589 4), adjacent to bore hole DSDP595, which contradicts the 84.4 Ar/Ar age of Mortimer et al.  
590 (2019).

591         We reconstruct the start of spreading in both basins at 120 Ma (Fig. 6B), following  
592 Chandler et al. (2012), similar to Seton et al. (2012) and Müller et al. (2019). For the Osbourn  
593 Trough, we use rotation poles of Chandler et al. (2012) to reconstruct the spreading history, but  
594 we incorporate the new constraints from Mortimer et al. (2019) of spreading until 79 Ma rather

595 than the contested, New Zealand geology-based 86 Ma estimate of Worthington et al. (2006)  
596 that is used in Seton et al. (2012) and Müller et al. (2019). We note that the age for the end of  
597 Osbourn Trough spreading may change in the future if more reliable radiometric dating of the  
598 Osbourn Basin becomes available, and we will discuss below what difference a different age  
599 would make for the estimate for subduction arrest at the New Zealand margin. For the Ellice  
600 Basin, we use the Chandler et al. (2012) rotation pole for the Ontong Java-Manihiki fit at 120 Ma  
601 and the rotation poles of Benyshek et al. (2019) for subsequent opening, with spreading ending  
602 at 90 Ma.

603 The contemporaneous opening of the Ellice Basin and Osbourn Trough requires that a  
604 mid-ocean ridge existed between the Hikurangi and Pacific plates (Fig. 6B-E). The rate and  
605 direction of spreading along this ridge follows from the Pacific-Manihiki and Manihiki-  
606 Hikurangi reconstructions. This spreading ridge, as well as the Pacific-Manihiki-Hikurangi triple  
607 junction was lost to subduction at the Tonga-Kermadec-Hikurangi subduction zone during the  
608 Cenozoic (Fig. 6E-J).

609

#### 610 **4.2.3. Seafloor fabric**

611 To the east of the Manihiki and Hikurangi plates, Seton et al. (2012) identified two more  
612 daughter plates of the Phoenix Plate: Chasca and Catequil. We continue using the name Chasca  
613 Plate, but the Catequil Plate of Seton et al. (2012) is the same as the Aluk Plate in our  
614 reconstruction. We prefer the name Aluk Plate, because it is the established name for the  
615 remnant of this plate whose lithosphere remains in the southeast Pacific today. As with Seton et  
616 al. (2012), we derive the former existence of the Chasca and Aluk plates from seafloor fabric and  
617 marine magnetic anomaly identifications.

618 The pre-83.7 Ma existence of the Aluk Plate follows from trends in the seafloor fabric  
619 east of the Osbourn Trough. The extinct Osbourn Trough spreading center can be followed  
620 eastwards until longitude 165°W, where it suddenly stops (Fig. 8). North and south of the  
621 Osbourn Trough abyssal hill trends are WNW-ESE for the older part of the basin, and E-W for  
622 the youngest part (Downey et al., 2007, see also their Fig. 6). These abyssal hill trends, together  
623 with NNE-SSW trending fracture zones constrains the NNE-SSW to N-S spreading direction of  
624 the Hikurangi Plate relative to the Manihiki Plate. This trend in seafloor fabric that formed at the  
625 Osbourn Trough is delineated by the NNE-SSW trending Manihiki Scarp and the West Wishbone  
626 Ridge, clear traces in the ocean floor (Fig. 8). East of the Manihiki Scarp and West Wishbone  
627 Ridge, abyssal hills are trending ENE-WSW (Downey et al., 2007, their Fig. 6) and fracture zones  
628 are trending NNW-SSE (Fig. 8). This suggests that the oceanic crust here formed at a different  
629 spreading center, between different plates (Downey et al., 2007). We suggest here that this part  
630 of oceanic crust formed through spreading between the Manihiki and Aluk plates, both

631 daughters of the Phoenix Plate. There is no remnant of an extinct spreading ridge preserved in  
632 this part of the Pacific Plate, which suggests that all oceanic crust preserved here formed as part  
633 of the Manihiki Plate (e.g., Seton et al., 2012). As Manihiki was incorporated into the Pacific Plate  
634 at c. 90 Ma (Benyshek et al., 2019), the Manihiki-Aluk ridge became the Pacific-Aluk ridge at this  
635 time. The location of the Pacific-Aluk Ridge is constrained after 83.7 Ma by marine magnetic  
636 anomalies preserved on the Pacific Plate (Fig. 4 and 6E; see also section 4.1) (Cande et al., 1995;  
637 Larter et al., 2002; Eagles et al., 2004; Wobbe et al., 2012). The direction of spreading between  
638 the Manihiki/Pacific and Aluk plates follows from the NNW-SSE directed fracture zones that are  
639 preserved on the Pacific Plate (Fig. 8). The average rate of Manihiki-Aluk spreading follows from  
640 the 120 Ma break-up configuration of the Phoenix Plate into these plates and the chron C34y  
641 (83.7 Ma) location of the Aluk-Pacific ridge, which is constrained by marine magnetic anomalies  
642 on the Pacific Plate (Larter et al., 2002; Eagles et al., 2004). We reconstruct a constant spreading  
643 rate in this 120-83.7 Ma period.

644         The nature of the plate boundary between the Aluk and Hikurangi plates follows from  
645 the reconstruction of the Hikurangi and Aluk plates relative to the Manihiki Plate. In our  
646 reconstruction, Aluk-Manihiki spreading occurred at a higher rate than Hikurangi-Manihiki  
647 spreading (~8.5 cm/yr and ~4.5 cm/yr half-spreading rate, respectively) (Fig. 6B-D). As a  
648 result, between 120 and 110 Ma, the plate boundary between the Aluk and Hikurangi plates was  
649 a right-lateral transform fault northeast of the Hikurangi Plateau, forming the West Wishbone  
650 Ridge. After 110 Ma, some extension occurred between the Aluk and Hikurangi plates east of the  
651 Hikurangi Plateau, accommodated by a mid-ocean ridge. South of the Hikurangi Plateau, the  
652 plate boundary between the Hikurangi and Aluk plates was a mid-ocean ridge from 120 Ma  
653 until its subduction below the Zealandia margin around 100-90 Ma (Fig. 6B-C and 7).

654         From the northeast corner of the Manihiki Plateau towards the south, there is a clear  
655 trace in the seafloor fabric (Fig. 8). This feature has been identified as a trace of a former triple  
656 junction (Larson and Chase, 1972), and was named the Tongareva triple junction (Larson et al.,  
657 2002). It was previously suggested that the Tongareva triple junction formed the junction  
658 between the Pacific, Farallon, and Phoenix plates (e.g., Larson et al., 2002; Viso et al., 2005;  
659 Hochmuth and Gohl, 2017). We instead infer that the Tongareva triple junction formed the  
660 junction between Manihiki, Chasca and Aluk plates, until c. 90 Ma, when Manihiki merged with  
661 the Pacific Plate. Between 90 and 83.7 Ma, the Tongareva triple junction was the junction of the  
662 Pacific, Chasca and Aluk plates, after which it became the triple junction between Pacific,  
663 Farallon and Aluk plates when Chasca was captured by Farallon (Fig. 6B-F).

664         The existence of the Chasca Plate follows from rift structures on the northeast margin of  
665 the Manihiki Plateau (Fig. 8) (Larson et al., 2002; Viso et al., 2005). It was previously suggested  
666 that this fragment was incorporated into the Farallon Plate at 110 Ma (Hochmuth and Gohl,

2017). The location of the Farallon Plate relative to the Pacific Plate is constrained by marine magnetic anomalies of chrons C34y (83.7) and M0 (121.4). Attaching a fragment of oceanic crust that formed east of the Manihiki Plateau to the Farallon Plate at 110 Ma, however, leads to convergence along the southeast margin of the Manihiki Plateau. This convergence is contradicted by the existence of the Tongareva triple junction trace, as described above. Instead, we reconstruct independent motion of the Chasca Plate until 83.7 Ma. The capture of the Chasca Plate by the Farallon Plate, which resulted from the inactivation of the transform fault (Clipperton Fracture Zone) that separated the Chasca and Farallon plates, may have occurred a few millions of years earlier. This would require higher Chasca – Manihiki/Pacific spreading rates, but these are unknown. We therefore choose to reconstruct the capture at the time of C34y (83.7 Ma), as this marine magnetic anomaly provides the first positive evidence that the Chasca plate was captured. Seton et al. (2012) and Chandler et al. (2012) incorporate the Chasca Plate into the Farallon Plate a few million years earlier at 86 Ma, contemporaneous with the cessation of Osborn Trough spreading in their model (see section 4.2.2).

We reconstruct the start of Chasca – Manihiki motion at 120 Ma, the same time as the onset of spreading between the other daughters of the Phoenix Plate (Chandler et al., 2012). Rotation poles of the Chasca Plate relative to the Manihiki Plate are calculated in GPlates. In our reconstruction, we ensure that early motion of the Chasca Plate follows the trend of the curved rift structures at the NE Manihiki margin (Fig. 8). In addition, we assume that the Pacific-Farallon ridge at 83.7 Ma formed at the location of the Pacific-Chasca ridge, after Manihiki was captured by the Pacific Plate at 90 Ma (Benyshek et al., 2019) and Chasca was captured by Farallon.

The rotation poles for the reconstruction of the Ellice Basin include a rotation of the Manihiki Plate relative to the Pacific Plate between 102 and 98 Ma, based on a change in fracture zone orientation in the Ellice Basin from ~E-W to WNW-ESE (Taylor, 2006; Chandler et al., 2012; Benyshek et al., 2019). As the Chasca Plate is reconstructed relative to the Manihiki Plate in our plate circuit, the rotation modeled by Benyshek et al. (2019) also results in a rotation of the Chasca Plate. This in turn leads to convergence at the Chasca-Farallon plate boundary that at that time was still located at the latitude of northern South America. This rotation of the Chasca Plate coincides with the estimated timing of subduction initiation at the western Caribbean plate boundary of modern Central America (Whattam and Stern, 2015; Boschman et al., 2019), which at 100 Ma was still located far west within the eastern Panthalassa realm (e.g., Pindell and Kennan, 2009; Boschman et al., 2014). Rotation of the Manihiki Plate may thus have resulted in subduction initiation at the future western Caribbean plate boundary.

702

## 703        **5. Discussion**

704        The kinematic constraints reviewed in section 4 lead to a plate kinematic evolution from 150  
705        Ma onward as portrayed in Fig. 6, and in snapshots highlighting the final stages of subduction in  
706        Fig. 7. We provide GPlates reconstruction files and an animation of the reconstruction in the  
707        supplementary information. Below, we discuss uncertainties in our reconstruction, offer  
708        interpretations of possible dynamic drivers of plate reorganizations, and evaluate until when  
709        convergence along the Gondwana margin must have continued. Finally, we discuss how  
710        differences between plate kinematics and geology-based interpretations may be reconciled, and  
711        what opportunities our reconstruction provides for future geological research.

712

### 713                    **5.1 Dating the end of convergence across the Gondwana margins**

714                During the Paleozoic and Mesozoic, the vast Phoenix Plate occupied large parts of the  
715        south Panthalassa Ocean. After the birth of the Pacific Plate around 190 Ma (Seton et al., 2012;  
716        Boschman and Van Hinsbergen, 2016), the Phoenix Plate formed spreading ridges with the  
717        Pacific, Izanagi/Izanami and Farallon plates. Subduction at the Gondwana margin of South  
718        America, Antarctica, and Australia/Zealandia is not controversial, although more plates may  
719        have been involved between the Phoenix Plate and the Gondwana margin (e.g., Boschman et al.,  
720        2021a). Our reconstruction from 150 Ma until the 125-120 Ma emplacement of the Ontong Java  
721        Nui LIP, placed in the Pacific hotspot reference frame of Torsvik et al. (2019) and the Indo-  
722        Atlantic slab-fitted frame of Van der Meer et al. (2010) straightforwardly shows convergence of  
723        Phoenix in the west, south, and east, consistent with geological records from South America,  
724        Antarctica, and Zealandia (Mortimer et al., 2014; Burton-Johnson and Riley, 2015; Pepper et al.,  
725        2016; Jordan et al., 2020; Maurizot et al., 2020b). Along the eastern margin of the southern  
726        Pacific, convergence and subduction continue today (Fig. 1). Conversely, convergence ceased  
727        along the southern and western margins in the Late Cretaceous, which was followed by re-  
728        initiation of subduction in the west during the Cenozoic (e.g. Seton et al., 2012; Van de Lagemaat  
729        et al., 2018a). In this section, we establish until when, according to plate kinematic constraints,  
730        subduction continued. In addition, we examine whether the choice of mantle reference frame is  
731        of influence on this age estimation.

732                It is well agreed upon that a subduction zone was present along the entire East  
733        Gondwana margin, from the Antarctic Peninsula until at least New Caledonia, until 105 Ma  
734        (Bradshaw, 1989; Luyendyk, 1995; Maurizot et al., 2020b; Gardiner et al., 2021). But after 105-  
735        100 Ma, when some models that are based on onshore geology (e.g., the onset of continental  
736        extension and the change in geochemistry of magmatism) argue for the cessation of subduction  
737        along the Zealandia sector of East Gondwana (Bradshaw, 1989; Davy et al., 2008; Crampton et  
738        al., 2019; Mortimer et al., 2019). However, our plate reconstruction shows that convergence at

739 the Zealandia and Antarctic margins continued, until at least 90 Ma and possibly until 85 Ma  
740 (Fig. 9). In our updated plate kinematic model, the timing of the end of convergence is  
741 dependent on two variables: the reconstruction of Osbourn Trough spreading and the choice of  
742 Indo-Atlantic mantle reference frame for East Gondwana. We only use the Pacific mantle  
743 reference frame of Torsvik et al. (2019), because they showed that previous Pacific reference  
744 frames are flawed. In all Indo-Atlantic mantle reference frames, convergence continues until the  
745 cessation of Osbourn Trough spreading; that is, until 79 Ma in our reconstruction following  
746 Mortimer et al. (2019). This reconstruction of the Osbourn Trough leads to c. 1500-2000 km of  
747 convergence between the Hikurangi Plate and the Gondwana margin between 100 and 79 Ma,  
748 depending on the reference frame (Fig. 9). If future radiometric dating of dredge samples would  
749 suggest an older age for the end of Osbourn Trough spreading, the convergence between the  
750 Hikurangi Plate and the East Gondwana margin would simply be accommodated by higher rates  
751 of spreading and subduction between 120 Ma and any new and reliable date suggested. Even if  
752 Osbourn Trough spreading had already ceased by 101 Ma, as interpreted by Zhang and Li  
753 (2016), there would still have been 800-1100 km of post-100 Ma convergence between the  
754 Pacific Plate and the Zealandia margin (Fig. 9). In this scenario, convergence at the Zealandia  
755 margin continued until c. 90 Ma, applying the reference frames of Torsvik et al. (2008) or  
756 Doubrovine et al. (2012), or continued until c. 84 Ma (when the Campbell plateau became  
757 incorporated in the Pacific Plate) in applying the slab frame of Van der Meer et al. (2010) or the  
758 hotspot reference frame of O'Neill et al. (2005).

759         The Hikurangi-Pacific ridge formed a triple junction with the subduction zone located  
760 along the margin of East Gondwana, in the vicinity of the Norfolk Ridge (Fig. 6 and 7). North of  
761 this Hikurangi-Pacific-Gondwana triple junction, the rate and amount of convergence at the East  
762 Gondwana margin were not influenced by spreading at the Osbourn Trough, as the Pacific Plate  
763 directly subducted below the Norfolk Ridge. The precise location of this triple junction, where  
764 the Pacific-Hikurangi ridge subducted below eastern Gondwana, is uncertain, as it has  
765 subsequently been consumed at the Cenozoic Tonga-Kermadec and New Caledonia trenches. In  
766 our reconstruction, after 95 Ma we place this triple junction just south of New Caledonia (Fig. 6  
767 and 7), which results from the assumption of symmetric spreading between the Pacific and  
768 Hikurangi plates between 120 and 79 Ma (see section 4.2.2). The relative motion between the  
769 Pacific Plate and the Norfolk Ridge north of the Pacific-Hikurangi-Gondwana triple junction is  
770 convergent in all reference frames until at least 90 Ma. In the hotspot reference frames of O'Neill  
771 et al. (2005), Torsvik et al. (2008), and Doubrovine et al. (2012), convergence north of the  
772 Hikurangi-Pacific-Gondwana triple junction ends at 90 Ma (Fig. 9). In the slab-fitted mantle  
773 reference frame of Van der Meer et al. (2010), convergence between the Pacific Plate and the

774 Norfolk Ridge continues until 85 Ma. Subduction south of the New Caledonia sector of the East  
775 Gondwana margin thus continued until 90-85 Ma (Fig. 9).

776 In an attempt to reconcile geological (on-land) interpretations of cessation of  
777 subduction in New Zealand with oceanic plate reconstructions, Mortimer et al. (2019) proposed  
778 a solution to avoid convergence beyond 100 Ma at the Zealandia margin. In this scenario, the  
779 Hikurangi Plateau arrives in the trench at 100 Ma, and the Manihiki and Ontong Java plateaus  
780 move northwards relative to the margin between 100 and 79 Ma. However, this model places  
781 the Pacific plate mosaic ~2250 km farther to the South at 100 Ma than suggested by the hotspot  
782 frame of Torsvik et al. (2019) (Fig. 10), which is well beyond the uncertainty in the hotspot  
783 model of a few hundred km. The solution of Mortimer et al. (2019) is therefore unrealistic; it  
784 would require an absolute hotspot wander between 100 and 90-85 Ma of 10-20 cm/yr, for all  
785 hotspots below the Pacific Plate, for which there is no evidence, and which is two orders of  
786 magnitude faster than typical hotspot motions (e.g., Doubrovine et al., 2012). In addition, we  
787 tested whether the latest and highest-detail published isochron sets from the South Pacific  
788 realm change the age for the end of convergence across the Gondwana margin that followed  
789 from widely used global plate models (e.g., Seton et al., 2012; Müller et al., 2019). And while our  
790 updated model differs in detail, for instance in the reconstruction of plates and plate motions in  
791 lithosphere that was lost to subduction, the conclusions from those global models are  
792 robust: Plate kinematic models leave no room for a cessation of subduction along the Zealandia  
793 margin at 100 Ma or before; instead, convergence between the Phoenix Plate's daughters and  
794 the East Gondwana margin must have continued until at least 90-85 Ma. Below the New Zealand  
795 margin, convergence likely continued even longer if spreading in the Osborn Trough continued  
796 beyond 85 Ma (e.g., 79 Ma according to Mortimer et al., 2019).

797

## 798 **5.2 Reconciling ongoing convergence after 100 Ma with the geology of** 799 **Zealandia**

800 Our plate kinematic reconstruction requires that convergence, and by inference  
801 subduction, continued until at least 90 Ma along the entire East Gondwana margin, and possibly  
802 until 79 Ma below New Zealand and Chatham Rise. While our reconstruction is easily reconciled  
803 with the geology of New Caledonia, where subduction-related accretion and magmatism  
804 continued until c. 90 Ma (Cluzel et al., 2010; Maurizot et al., 2020b), it conflicts with the  
805 common interpretation based on geological observations from New Zealand that subduction  
806 there ceased at 105-100 Ma. The observations from New Zealand thus require an alternative  
807 explanation.

808 The first often-cited argument for subduction cessation at 105-100 Ma is the timing of  
809 the onset of extension that is recognized in the geology of New Zealand (Bradshaw, 1989;

810 Tulloch and Kimbrough, 1989; Field and Uruski, 1997; Laird and Bradshaw, 2004; Crampton et  
811 al., 2019), for example in the Canterbury Basin (Barrier et al., 2020). However, extension in the  
812 upper plate above an active subduction zone is common, as evidenced by many intra- and back-  
813 arc basins across the world. In fact, extension is presently occurring within the Taupo Volcanic  
814 Zone in North Island New Zealand, above the Hikurangi subduction zone (e.g., Villamor and  
815 Berryman, 2001). In addition, neither numerical models (e.g., Van Hunen and Allen, 2011;  
816 Duretz et al., 2014) nor geological observations (Wortel and Spakman, 2000; Webb et al., 2017;  
817 Qayyum et al., 2022) suggest a systematic relationship between slab break-off and upper plate  
818 extension. It is even questionable whether the onset of extension in East Gondwana, which is  
819 recorded from the West Antarctic Rift System to the Tasman Sea region (Gaina et al., 1998;  
820 Behrendt, 1999; Fitzgerald, 2002; Raza et al., 2009; Cluzel et al., 2012; Spiegel et al., 2016;  
821 Jordan et al., 2020), is directly governed by subduction termination, or related to the intra-  
822 continental forces that governed Gondwana breakup. In any case, extension in the Gondwana  
823 margin does not necessitate slab break-off and does not exclude ongoing subduction.

824         The geological interpretation of the cessation of subduction around 105 – 100 Ma is  
825 further inferred from interpretation of the geodynamic setting that caused a change in  
826 geochemical signature of magmatism in New Zealand. Although the youngest age of ‘normal’  
827 subduction-related I-type magmatism in New Zealand was dated as 128 Ma (Tulloch and  
828 Kimbrough, 2003), the 131-105 Ma adakitic magmatism is also considered to be related to  
829 ongoing subduction (Tulloch et al., 2009). The subsequent onset of A-type magmatism around  
830 100 Ma is widely regarded as signaling the end of subduction (Tulloch et al., 2009). However,  
831 the increase in A-type magmatism is interpreted as the result of thinning of the continental  
832 crust of Zealandia during extension, which caused less crustal contamination of the igneous  
833 rocks (Tulloch et al., 2009), indicating that these interpretations were made under the  
834 assumption that subduction ended around 100 Ma, and no alternative causes were explored.

835         While A-type magmatism is generally interpreted as occurring in the absence of  
836 subduction (Loiselle and Wones, 1979), such magmas have also been found in active margin  
837 settings, for example related to the arrival of a spreading ridge and the influx of sub-slab mantle  
838 to the former wedge (e.g. Zhao et al., 2008; Karsli et al., 2012; Li et al., 2012). We here suggest  
839 that the transition to A-type magmatism in New Zealand may also be explained by arrival of a  
840 spreading ridge. As explained in section 4.2.3, the plate boundary between the Hikurangi and  
841 Aluk plates was likely a spreading ridge south of the Hikurangi Plateau. Our reconstruction  
842 predicts that this spreading ridge subducted around 100 Ma below New Zealand (Fig. 7 and 11).  
843 The progressive arrival of successively younger oceanic crust before arrival of the spreading  
844 ridge may then explain the 128-105 Ma adakitic magmatism, which is often related to the  
845 subduction of young oceanic crust (Tulloch and Rabone, 1993).



846 In summary, geological and geochemical interpretations made for New Zealand do not  
847 require that subduction ended during c. 105-100 Ma (Fig. 7 and 11). Alternative structural and  
848 stratigraphic arguments for the forearc region of New Zealand (Mazengarb and Harris, 1994;  
849 Kamp, 1999, 2000; Gardiner and Hall, 2021) are straightforwardly reconciled with ongoing  
850 subduction, along with geochemical arguments for the composition of magmatic rocks, which do  
851 not exclude ongoing subduction.

852

### 853 **5.3 Causes for the end of subduction**

854 Why subduction stopped at the margin of East Gondwana in the Cretaceous is puzzling.  
855 Explanations for this cessation have so far mostly focused on regional geological features, such  
856 as the arrival of a mid-ocean ridge in the trench (Luyendyk, 1995; Bradshaw, 1989; Matthews et  
857 al., 2012). The arrival of a mid-ocean ridge in a subduction zone may indeed change the nature  
858 of a plate boundary and trigger slab break-off. The nature of the plate boundary that follows  
859 upon ridge arrival commonly depends on the relative motion between the original overriding  
860 plate and the plate that was formerly spreading with the original down-going plate. For  
861 example, west of the active trench below the Antarctic Peninsula, marine magnetic anomalies  
862 young from the ocean towards West Antarctica. This shows that subduction below the Antarctic  
863 Peninsula indeed ceased due to the arrival of the Aluk-West Antarctica ridge at the trench below  
864 West Antarctica, after which relative motion ceased (Eagles, 2004). However, the Hikurangi-  
865 Pacific ridge did not subduct parallel to the trench but subducted at an angle to it (Fig. 6C-E and  
866 7A-D). Moreover, until the ~84 Ma change in absolute plate motion of the Pacific Plate, the  
867 whole Panthalassa mosaic was converging with the East Gondwana margin, which means that  
868 subduction continued after the arrival of the Hikurangi-Aluk spreading ridge. More importantly,  
869 the newly formed Pacific-Antarctic Ridge did not replace the former subduction zone but cut  
870 through the suture and formed at a completely different location (Fig. 6D-E and 7C-D). Ridge  
871 arrival is thus not a likely candidate to explain the end of subduction.

872 A second hypothesis for the end of subduction below the Zealandia margin of East  
873 Gondwana is the arrival of the Hikurangi Plateau in the trench (e.g., Billen and Stock, 2000; Davy  
874 et al., 2008, Davy, 2014; Timm et al., 2014; Reyners et al., 2017; Mortimer et al., 2019). However,  
875 the Hikurangi Plateau only represents a small portion of the Pacific Plate and only a short length  
876 of the trench. If a transform fault could be demonstrated to have bounded the western side of  
877 the Hikurangi Plateau, subduction could have continued below the North Island and New  
878 Caledonia sections. Moreover, while plateau arrivals at intra-oceanic trenches may cause a  
879 polarity reversal (and ongoing subduction), e.g., during the arrival of the Ontong Java Plateau at  
880 the Vitiaz trench triggering the formation of the New Hebrides trench and the South Solomon  
881 trench (Auzende et al., 1995; Petterson et al., 1997; Quarles van Ufford and Cloos, 2005; Knesel

882 et al., 2008; Lallemand and Arcay, 2021), there is no record of LIP arrival at a trench causing  
883 subduction cessation or a plate reorganization on the scale as observed here. Instead, LIP  
884 subduction is physically straightforward, even though it may cause shallow dipping slabs (e.g.,  
885 Yang et al., 2020; Liu et al., 2021). LIP subduction has, for example, been ongoing in the  
886 Maracaïbo trench of the southern Caribbean region for more than 50 Ma (White et al., 1999;  
887 Boschman et al., 2014), and even the Hikurangi Plateau itself is subducting today at the  
888 Hikurangi trench (Collot et al., 1998; Reyners et al., 2011; Fig. 1). Therefore, while the  
889 preservation of the Hikurangi Plateau at the Gondwana margin may suggest that it played a role  
890 in determining where the slab broke, it is an unlikely trigger for the cessation of subduction  
891 along the entire East Gondwana margin.

892         Instead, we consider it most likely that the end of subduction in the Zealandia sector of  
893 East Gondwana was governed by a change in relative plate motion between the Pacific Plate and  
894 East Gondwana (Rey and Müller, 2010). More analysis of the driving forces of the Pacific Plate  
895 and the Pacific plate mosaic as a whole, not only of local features on the southernmost Pacific  
896 Plate could usefully be undertaken. In the East Asia region, below South China, we note that  
897 subduction along the continental margin suddenly stopped at around 90-80 Ma (e.g., Cui et al.,  
898 2021). Also, in the North Pacific realm there were prominent changes in plate boundary  
899 configuration around 90-85 Ma, including the formation of the Kula plate (Engebretson et al.,  
900 1985; Wright et al., 2016), and initiation of intra-oceanic subduction below the Olyutorsky and  
901 Kronotsky arcs (Konstantinovskaya, 2002; Shapiro and Solov'ev, 2009; Domeier et al., 2017;  
902 Vaes et al., 2019). An analysis of the causes of plate motion change that formed the prelude to  
903 the end of subduction below eastern Gondwana requires a detailed kinematic restoration of the  
904 plate boundary reorganization, particularly in the enigmatic transition between the Panthalassa  
905 and Tethyan domains of SE Asia, which is beyond the scope of this paper.

906

## 907 **5 Conclusions**

908 We have developed a kinematic reconstruction of the South Pacific and East Gondwana realms  
909 back to the Late Jurassic (150 Ma). Our aim was to reconstruct the evolution and destruction of  
910 the Phoenix Plate, and to reconcile the geological record of New Zealand with the end of  
911 Mesozoic subduction along the East Gondwana margin. From our reconstruction we conclude  
912 the following:

- 913 1) Resulting from the emplacement of Ontong Java Nui around 125-120 Ma, the Phoenix  
914 Plate broke into at least four plates: The Manihiki, Hikurangi, Chasca, and Aluk plates.  
915 During the Late Cretaceous, the Manihiki and Hikurangi plates were captured by the  
916 Pacific Plate, while Chasca was captured by the Farallon Plate. Only the Aluk Plate  
917 remained an independent tectonic plate into the Cenozoic.

- 918 2) Convergence occurred along the Gondwana margin until 90 or 85 Ma, depending on  
919 choice of mantle reference frame. This convergence occurred independent from  
920 spreading at the Osbourn Trough and required the presence of a subduction zone along  
921 the entire Zealandia margin until at least 90 Ma and possibly until 85 Ma.
- 922 3) Subduction in the New Caledonia region ceased at c. 90 to 85 Ma, but convergence of the  
923 Hikurangi Plate with the Chatham Rise must have continued until the cessation of  
924 spreading at the Osbourn Trough, recently tentatively estimated at 79 Ma.
- 925 4) The cessation of subduction of the Hikurangi Plate along the entire East Gondwana  
926 margin was probably a result of a change in Pacific-Gondwana relative plate motion.  
927 This was not due to the arrival of the small Hikurangi Plateau compared with the East  
928 Gondwana subduction system.
- 929 5) The 105-100 Ma structural changes within the crust of the overriding New Zealand  
930 continental plate may have resulted from subduction of the Aluk-Hikurangi ridge, rather  
931 than from the cessation of subduction at the East Gondwana margin.
- 932 6) Geological expressions in the overriding plate may be misleading when used to interpret  
933 subduction zone dynamics. While a geological record in the overriding plate may  
934 provide evidence for the presence of subduction, absence of such evidence should not be  
935 interpreted as conclusive evidence for the absence of subduction.

936

### 937 **Acknowledgements**

938 DJJvH and SHAvdL acknowledge NWO Vici grant 865.17.001. PJJk acknowledges funding from  
939 the New Zealand Government (MBIE Contract: CONT-42907-EMTR-UOW).

940

### 941 **References**

- 942 Adams, C. J., Campbell, H. J., Graham, I. J., & Mortimer, N. (1998). Torlesse, Waipapa and Caples  
943 suspect terranes of New Zealand: integrated studies of their geological history in relation  
944 to neighbouring terranes. *Episodes*, 21, 235-240.
- 945 Adams, C. J., Campbell, H. J., & Griffin, W. L. (2007). Provenance comparisons of Permian to  
946 Jurassic tectonostratigraphic terranes in New Zealand: perspectives from detrital zircon  
947 age patterns. *Geological Magazine*, 144(4), 701-729.
- 948 Adams, C. J., Mortimer, N., Campbell, H. J., & Griffin, W. L. (2013). The mid-Cretaceous transition  
949 from basement to cover within sedimentary rocks in eastern New Zealand: evidence from  
950 detrital zircon age patterns. *Geological Magazine*, 150(3), 455-478.
- 951 Amante, C. and Eakins, B.W. (2009). ETOPO1 1 Arc-Minute Global Relief Model: Procedures,  
952 Data Sources and Analysis. NOAA Technical Memorandum NESDIS NGDC-24. National  
953 Geophysical Data Center, NOAA. doi:10.7289/V5C8276M

- 954 An, M., Wiens, D. A., Zhao, Y., Feng, M., Nyblade, A. A., Kanao, M., Li, Y., Maggi, A., & L ev eque, J. J.  
955 (2015). S-velocity model and inferred Moho topography beneath the Antarctic Plate from  
956 Rayleigh waves. *Journal of Geophysical Research: Solid Earth*, 120(1), 359-383.
- 957 Atwater, T., & Severinghaus, J. (1989). Tectonic maps of the northeast Pacific. In *The Eastern*  
958 *Pacific Ocean and Hawaii*, E. L. Winterer, Donald M. Hussong, Robert W. Decker (Eds).  
959 Geological Society of America. <https://doi.org/10.1130/DNAG-GNA-N.15>
- 960 Auzende, J. M., Pelletier, B., & Eissen, J. P. (1995). The North Fiji Basin geology, structure, and  
961 geodynamic evolution. In *Backarc Basins* (pp. 139-175). Springer, Boston, MA.
- 962 Barckhausen, U., Ranero, C. R., von Huene, R., Cande, S. C., & Roeser, H. A. (2001). Revised  
963 tectonic boundaries in the Cocos Plate off Costa Rica: Implications for the segmentation of  
964 the convergent margin and for plate tectonic models. *Journal of Geophysical Research:*  
965 *Solid Earth*, 106(B9), 19207-19220.
- 966 Barckhausen, U., Ranero, C. R., Cande, S. C., Engels, M., & Weinrebe, W. (2008). Birth of an  
967 intraoceanic spreading center. *Geology*, 36(10), 767-770.
- 968 Barker, P. F. (1982). The Cenozoic subduction history of the Pacific margin of the Antarctic  
969 Peninsula: ridge crest-trench interactions. *Journal of the Geological Society*, 139(6), 787-  
970 801.
- 971 Barrier, A., Nicol, A., Browne, G. H., & Bassett, K. N. (2020). Late Cretaceous coeval multi-  
972 directional extension in South Zealandia: Implications for eastern Gondwana  
973 breakup. *Marine and Petroleum Geology*, 118, 104383.
- 974 Behrendt, J. C. (1999). Crustal and lithospheric structure of the West Antarctic Rift System from  
975 geophysical investigations—a review. *Global and Planetary Change*, 23(1-4), 25-44.
- 976 Benyshek, Elizabeth K., Paul Wessel, and Brian Taylor. "Tectonic Reconstruction of the Ellice  
977 Basin." *Tectonics* 38.11 (2019): 3854-3865.
- 978 Billen, M. I., & Stock, J. (2000). Morphology and origin of the Osbourn Trough. *Journal of*  
979 *Geophysical Research: Solid Earth*, 105(B6), 13481-13489.
- 980 Bird, P. (2003). An updated digital model of plate boundaries. *Geochemistry, Geophysics,*  
981 *Geosystems*, 4(3).
- 982 Boschman, L. M., van Hinsbergen, D. J., Torsvik, T. H., Spakman, W., & Pindell, J. L. (2014).  
983 Kinematic reconstruction of the Caribbean region since the Early Jurassic. *Earth-Science*  
984 *Reviews*, 138, 102-136.
- 985 Boschman, L. M., & Van Hinsbergen, D. J. J. (2016). On the enigmatic birth of the Pacific Plate  
986 within the Panthalassa Ocean. *Science Advances*, 2(7), e1600022.
- 987 Boschman, L. M., Van Hinsbergen, D. J. J., Langereis, C. G., Flores, K. E., Kamp, P. J. J., Kimbrough,  
988 D. L., Ueda, H., Van de Lagemaat, S. H. A., Van der Wiel, E. & Spakman, W. (2021a).

- 989           Reconstructing lost plates of the panthalassa ocean through Paleomagnetic data from  
990           circum-pacific accretionary orogens. *American Journal of Science*, 321(6), 907-954.
- 991 Boschman, L. M., van Hinsbergen, D. J., & Spakman, W. (2021b). Reconstructing Jurassic-  
992           Cretaceous Intra-Oceanic Subduction Evolution in the Northwestern Panthalassa Ocean  
993           Using Ocean Plate Stratigraphy From Hokkaido, Japan. *Tectonics*, 40(8), e2019TC005673.
- 994 Boyden, J. A., Müller, R. D., Gurnis, M., Torsvik, T. H., Clark, J. A., Turner, M., Ivey-Law, H., Watson,  
995           R. J., & Cannon, J. S. (2011). Next-generation plate-tectonic reconstructions using GPlates.
- 996 Bradshaw, J. D. (1989). Cretaceous geotectonic patterns in the New Zealand  
997           region. *Tectonics*, 8(4), 803-820. <https://doi.org/10.1029/TC008i004p00803>
- 998 Burton-Johnson, A., & Riley, T. R. (2015). Autochthonous v. accreted terrane development of  
999           continental margins: a revised in situ tectonic history of the Antarctic Peninsula. *Journal of*  
1000           *the Geological Society*, 172(6), 822-835.
- 1001 Campbell, M. J., Rosenbaum, G., Allen, C. M., & Mortimer, N. (2020). Origin of dispersed Permian-  
1002           Triassic fore-arc basin terranes in New Zealand: Insights from zircon  
1003           petrochronology. *Gondwana Research*, 78, 210-227.
- 1004 Cande, S. C., Herron, E. M., & Hall, B. R. (1982). The early Cenozoic tectonic history of the  
1005           southeast Pacific. *Earth and Planetary Science Letters*, 57(1), 63-74.
- 1006 Cande, S. C., Raymond, C. A., Stock, J., & Haxby, W. F. (1995). Geophysics of the Pitman Fracture  
1007           Zone and Pacific-Antarctic plate motions during the Cenozoic. *Science*, 270(5238), 947-  
1008           953.
- 1009 Cande, S. C., & Stock, J. M. (2004a). Pacific—Antarctic—Australia motion and the formation of  
1010           the Macquarie Plate. *Geophysical Journal International*, 157(1), 399-414.
- 1011 Cande, S. C., & Stock, J. M. (2004b). Cenozoic reconstructions of the Australia-new Zealand-south  
1012           Pacific sector of antarctica.
- 1013 Cande, S. C., Patriat, P., & Dymant, J. (2010). Motion between the Indian, Antarctic and African  
1014           plates in the early Cenozoic. *Geophysical Journal International*, 183(1), 127-149.
- 1015 Chandler, M. T., Wessel, P., Taylor, B., Seton, M., Kim, S. S., & Hyeong, K. (2012). Reconstructing  
1016           Ontong Java Nui: Implications for Pacific absolute plate motion, hotspot drift and true  
1017           polar wander. *Earth and Planetary Science Letters*, 331, 140-151.
- 1018 Cluzel, D., & Meffre, S. (2002). The Boghen terrane (New Caledonia, SW Pacific): a Jurassic  
1019           accretionary complex. Preliminary U-Pb radiochronological data on detrital  
1020           zircon. *Comptes Rendus Geoscience*, 334(11), 867-874.
- 1021 Cluzel, D., Adams, C. J., Meffre, S., Campbell, H., & Maurizot, P. (2010). Discovery of Early  
1022           Cretaceous rocks in New Caledonia: New geochemical and U-Pb zircon age constraints on  
1023           the transition from subduction to marginal breakup in the Southwest Pacific. *The Journal*  
1024           *of Geology*, 118(4), 381-397.

- 1025 Cluzel, D., Maurizot, P., Collot, J., & Sevin, B. (2012). An outline of the geology of New Caledonia;  
1026 from Permian-Mesozoic Southeast Gondwanaland active margin to Cenozoic obduction  
1027 and supergene evolution. *Episodes*, 35(1), 72-86.
- 1028 Choi, H., Kim, S. S., Dymant, J., Granot, R., Park, S. H., & Hong, J. K. (2017). The kinematic  
1029 evolution of the Macquarie Plate: A case study for the fragmentation of oceanic  
1030 lithosphere. *Earth and Planetary Science Letters*, 478, 132-142.
- 1031 Collot, J. Y., Lamarche, G., Wood, R. A., Deltail, J., Sosson, M., Lebrun, J. F., & Coffin, M. F. (1995).  
1032 Morphostructure of an incipient subduction zone along a transform plate boundary:  
1033 Puysegur Ridge and Trench. *Geology*, 23(6), 519-522.
- 1034 Collot, J. Y., & Davy, B. (1998). Forearc structures and tectonic regimes at the oblique subduction  
1035 zone between the Hikurangi Plateau and the southern Kermadec margin. *Journal of*  
1036 *Geophysical Research: Solid Earth*, 103(B1), 623-650.
- 1037 Cox, A., & Hart, R. B. (1986). Plate Tectonics: How It Works: Blackwell Scientific  
1038 Publications. Inc. Boston. 392 pp.
- 1039 Crampton, J. S., Mortimer, N., Bland, K. J., Strogon, D. P., Sagar, M., Hines, B. R., King, P. R., &  
1040 Seebeck, H. (2019). Cretaceous termination of subduction at the Zealandia margin of  
1041 Gondwana: The view from the paleo-trench. *Gondwana Research*, 70, 222-242.  
1042 <https://doi.org/10.1016/j.gr.2019.01.010>
- 1043 Crameri, F. (2018), Scientific colour maps. Zenodo. <http://doi.org/10.5281/zenodo.1243862>
- 1044 Crameri, F., G.E. Shephard, and P.J. Heron (2020), The misuse of colour in science  
1045 communication, Nature Communications, 11, 5444. doi: 10.1038/s41467-020-19160-7
- 1046 Croon, M. B., Cande, S. C., & Stock, J. M. (2008). Revised Pacific-Antarctic plate motions and  
1047 geophysics of the Menard Fracture Zone. *Geochemistry, Geophysics, Geosystems*, 9(7).
- 1048 Cui, Y., Shao, L., Li, Z. X., Zhu, W., Qiao, P., & Zhang, X. (2021). A Mesozoic Andean-type active  
1049 continental margin along coastal South China: New geological records from the basement  
1050 of the northern South China Sea. *Gondwana Research*, 99, 36-52.
- 1051 Davy, B., Hoernle, K., & Werner, R. (2008). Hikurangi Plateau: Crustal structure, rifted formation,  
1052 and Gondwana subduction history. *Geochemistry, Geophysics, Geosystems*, 9(7).  
1053 <https://doi.org/10.1029/2007GC001855>
- 1054 Davy, B. (2014). Rotation and offset of the Gondwana convergent margin in the New Zealand  
1055 region following Cretaceous jamming of Hikurangi Plateau large igneous province  
1056 subduction. *Tectonics*, 33(8), 1577-1595. <https://doi.org/10.1002/2014TC003629>
- 1057 DeMets, C., & Merkouriev, S. (2019). High-resolution reconstructions of South America plate  
1058 motion relative to Africa, Antarctica and North America: 34 Ma to present. *Geophysical*  
1059 *Journal International*, 217(3), 1821-1853.

- 1060 Domeier, M., Shephard, G. E., Jakob, J., Gaina, C., Doubrovine, P. V., & Torsvik, T. H. (2017).  
1061 Intraoceanic subduction spanned the Pacific in the Late Cretaceous–Paleocene. *Science*  
1062 *Advances*, 3(11), eaao2303.
- 1063 Doubrovine, P. V., Steinberger, B., & Torsvik, T. H. (2012). Absolute plate motions in a reference  
1064 frame defined by moving hot spots in the Pacific, Atlantic, and Indian oceans. *Journal of*  
1065 *Geophysical Research: Solid Earth*, 117(B9).
- 1066 Downey, N. J., Stock, J. M., Clayton, R. W., & Cande, S. C. (2007). History of the Cretaceous  
1067 Osborn spreading center. *Journal of Geophysical Research: Solid Earth*, 112(B4).
- 1068 Duretz, T., Gerya, T.V. and Spakman, W., 2014. Slab detachment in laterally varying subduction  
1069 zones: 3-D numerical modeling. *Geophysical Research Letters*, 41(6): 1951-1956.
- 1070 Eagles, G. (2004). Tectonic evolution of the Antarctic–Phoenix plate system since 15 Ma. *Earth*  
1071 *and Planetary Science Letters*, 217(1-2), 97-109.
- 1072 Eagles, G., Gohl, K., & Larter, R. D. (2004a). High-resolution animated tectonic reconstruction of  
1073 the South Pacific and West Antarctic Margin. *Geochemistry, Geophysics, Geosystems*, 5(7).
- 1074 Eagles, G., Gohl, K., & Larter, R. D. (2004b). Life of the Bellingshausen plate. *Geophysical Research*  
1075 *Letters*, 31(7).
- 1076 Eagles, G., & Scott, B. G. (2014). Plate convergence west of Patagonia and the Antarctic Peninsula  
1077 since 61 Ma. *Global and Planetary Change*, 123, 189-198.
- 1078 Eakins, B. W., & Lonsdale, P. F. (2003). Structural patterns and tectonic history of the Bauer  
1079 microplate, Eastern Tropical Pacific. *Marine Geophysical Researches*, 24(3), 171-205.
- 1080 Engebretson, D. C., Cox, A., & Gordon, R. G. (1985). Relative motions between oceanic and  
1081 continental plates in the Pacific basin. *GSA Special Papers* 206.  
1082 <https://doi.org/10.1130/SPE206>
- 1083 Field, B. D., & Uruski, C. I. (1997). *Cretaceous-Cenozoic geology and petroleum systems of the East*  
1084 *Coast region, New Zealand* (Vol. 1). Institute of Geological & Nuclear Sciences.
- 1085 Fitzgerald, P. A. U. L. (2002). Tectonics and landscape evolution of the Antarctic plate since the  
1086 breakup of Gondwana, with an emphasis on the West Antarctic Rift System and the  
1087 Transantarctic Mountains. *Royal Society of New Zealand Bulletin*, 35, 453-469.
- 1088 Gaina, C., Müller, D. R., Royer, J. Y., Stock, J., Hardebeck, J., & Symonds, P. (1998). The tectonic  
1089 history of the Tasman Sea: a puzzle with 13 pieces. *Journal of Geophysical Research: Solid*  
1090 *Earth*, 103(B6), 12413-12433.
- 1091 Galindo-Zaldívar, J., Gamboa, L., Maldonado, A., Nakao, S., & Bochu, Y. (2004). Tectonic  
1092 development of the Bransfield Basin and its prolongation to the South Scotia Ridge,  
1093 northern Antarctic Peninsula. *Marine Geology*, 206(1-4), 267-282.

- 1094 Gibbons, A. D., Barckhausen, U., Van Den Bogaard, P., Hoernle, K., Werner, R., Whittaker, J. M., &  
1095 Müller, R. D. (2012). Constraining the Jurassic extent of Greater India: Tectonic evolution  
1096 of the West Australian margin. *Geochemistry, Geophysics, Geosystems*, 13(5).
- 1097 Gardiner, N. P., & Hall, M. (2021). Discordant forearc deposition and volcanism preceding late-  
1098 Cretaceous subduction shutdown in Marlborough, north-eastern South Island, New  
1099 Zealand. *Earth-Science Reviews*, 214, 103530.
- 1100 Gardiner, N. P., Hall, M. W., & Cawood, P. A. (2021). A forearc stratigraphic response to  
1101 Cretaceous plateau collision and slab detachment, South Island, New  
1102 Zealand. *Tectonics*, 40(10), e2021TC006806.
- 1103 Gardiner, N. P., Hall, M., Frears, B. T., & Lovell, R. W. (2022). A stratigraphic record from syn to  
1104 post subduction sedimentation in Marlborough, New Zealand, and implications for  
1105 Gondwana breakup. *Marine and Petroleum Geology*, 136, 105472.
- 1106 Grobys, J. W., Gohl, K., & Eagles, G. (2008). Quantitative tectonic reconstructions of Zealandia  
1107 based on crustal thickness estimates. *Geochemistry, Geophysics, Geosystems*, 9(1).
- 1108 Granot, R., Cande, S. C., Stock, J. M., & Damaske, D. (2013). Revised Eocene-Oligocene kinematics  
1109 for the West Antarctic rift system. *Geophysical Research Letters*, 40(2), 279-284.
- 1110 Granot, R., & Dymant, J. (2018). Late Cenozoic unification of East and West Antarctica. *Nature*  
1111 *Communications*, 9(1), 1-10.
- 1112 Gurnis, M., Van Avendonk, H., Gulick, S. P., Stock, J., Sutherland, R., Hightower, E., Shuck, B., Patel,  
1113 J., Williams, E., Kardell, D., Herzig, E., Idini, B., Graham, K., Estep, J., & Carrington, L. (2019).  
1114 Incipient subduction at the contact with stretched continental crust: The Puysegur  
1115 Trench. *Earth and Planetary Science Letters*, 520, 212-219.
- 1116 Hall, R. (2002). Cenozoic geological and plate tectonic evolution of SE Asia and the SW Pacific:  
1117 computer-based reconstructions, model and animations. *Journal of Asian Earth*  
1118 *Sciences*, 20(4), 353-431.
- 1119 Handschumacher, D. W. (1976). Post-Eocene plate tectonics of the eastern Pacific. *The*  
1120 *Geophysics of the Pacific Ocean Basin and its Margin*, 19, 177-202.
- 1121 Herron, E.M. and Tucholke, B.E., 1976. Sea-floor magnetic patterns and basement structure in  
1122 the southeastern Pacific. In: C.D. Hollister, C. Craddock et al., Initial Reports of the Deep  
1123 Sea Drilling Project, 35. U.S. Govt. Printing Office, Washington, D.C. pp. 263-278.
- 1124 Herzer, R. H., Barker, D. H. N., Roest, W. R., & Mortimer, N. (2011). Oligocene-Miocene spreading  
1125 history of the northern South Fiji Basin and implications for the evolution of the New  
1126 Zealand plate boundary. *Geochemistry, Geophysics, Geosystems*, 12,  
1127 Q02004. <https://doi.org/10.1029/2010GC003291>



- 1128 Hochmuth, K., Gohl, K., & Uenzelmann-Neben, G. (2015). Playing jigsaw with large igneous  
1129 provinces—A plate tectonic reconstruction of Ontong Java Nui, West Pacific. *Geochemistry,*  
1130 *Geophysics, Geosystems, 16*(11), 3789-3807.
- 1131 Hochmuth, K., & Gohl, K. (2017). Collision of Manihiki Plateau fragments to accretional margins  
1132 of northern Andes and Antarctic Peninsula. *Tectonics, 36*(2), 229-240.
- 1133 Hoernle, K., Hauff, F., Van den Bogaard, P., Werner, R., Mortimer, N., Geldmacher, J., Garbe-  
1134 Schönberg, D., & Davy, B. (2010). Age and geochemistry of volcanic rocks from the  
1135 Hikurangi and Manihiki oceanic Plateaus. *Geochimica et Cosmochimica Acta, 74*(24), 7196-  
1136 7219.
- 1137 House, M. A., Gurnis, M., Kamp, P. J., & Sutherland, R. (2002). Uplift in the Fiordland region, New  
1138 Zealand: Implications for incipient subduction. *Science, 297*(5589), 2038-2041.
- 1139 Iaffaldano, G., Bodin, T., & Sambridge, M. (2012). Reconstructing plate-motion changes in the  
1140 presence of finite-rotations noise. *Nature communications, 3*(1), 1-6.
- 1141 Isozaki, Y., Maruyama, S., & Furuoka, F. (1990). Accreted oceanic materials in  
1142 Japan. *Tectonophysics, 181*(1-4), 179-205.
- 1143 Isozaki, Y., Aoki, K., Nakama, T., & Yanai, S. (2010). New insight into a subduction-related  
1144 orogen: A reappraisal of the geotectonic framework and evolution of the Japanese  
1145 Islands. *Gondwana Research, 18*(1), 82-105.
- 1146 Jordan, T. A., Riley, T. R., & Siddoway, C. S. (2020). The geological history and evolution of West  
1147 Antarctica. *Nature Reviews Earth & Environment, 1*(2), 117-133.
- 1148 Kamp, P. J. J. (1999). Tracking crustal processes by FT thermochronology in a forearc high  
1149 (Hikurangi margin, New Zealand) involving Cretaceous subduction termination and mid-  
1150 Cenozoic subduction initiation. *Tectonophysics, 307*(3-4), 313-343.
- 1151 Kamp, P. J. J. (2000). Thermochronology of the Torlesse accretionary complex, Wellington  
1152 region, New Zealand. *Journal of Geophysical Research: Solid Earth, 105*(B8), 19253-19272.
- 1153 Karsli, O., Caran, Ş., Dokuz, A., Çoban, H., Chen, B., & Kandemir, R. (2012). A-type granitoids from  
1154 the Eastern Pontides, NE Turkey: Records for generation of hybrid A-type rocks in a  
1155 subduction-related environment. *Tectonophysics, 530*, 208-224.
- 1156 Knesel, K. M., Cohen, B. E., Vasconcelos, P. M., & Thiede, D. S. (2008). Rapid change in drift of the  
1157 Australian plate records collision with Ontong Java plateau. *Nature, 454*(7205), 754-757.
- 1158 Konstantinovskaia, E. A. (2001). Arc-continent collision and subduction reversal in the Cenozoic  
1159 evolution of the Northwest Pacific: an example from Kamchatka (NE  
1160 Russia). *Tectonophysics, 333*(1-2), 75-94.
- 1161 Laird, M. G., & Bradshaw, J. D. (2004). The break-up of a long-term relationship: the Cretaceous  
1162 separation of New Zealand from Gondwana. *Gondwana Research, 7*(1), 273-286.
- 1163 [https://doi.org/10.1016/S1342-937X\(05\)70325-7](https://doi.org/10.1016/S1342-937X(05)70325-7)

- 1164 Lallemand, S. and Arcay, D. (2021). Subduction initiation from the earliest stages to self-  
1165 sustained subduction: Insights from the analysis of 70 Cenozoic sites. *Earth-Science*  
1166 *Reviews*, 221: 103779.
- 1167 Larson, R.L. (1997). Superplumes and ridge interactions between Ontong Java and Manihiki  
1168 plateaus and the Nova-Canton trough. *Geology*, 25(9): 779-782.
- 1169 Larson, R. L., & Chase, C. G. (1972). Late Mesozoic evolution of the western Pacific  
1170 Ocean. *Geological Society of America Bulletin*, 83(12), 3627-3644.
- 1171 Larson, R. L., Pockalny, R. A., Viso, R. F., Erba, E., Abrams, L. J., Luyendyk, B. P., Stock, J. M., &  
1172 Clayton, R. W. (2002). Mid-Cretaceous tectonic evolution of the Tongareva triple junction  
1173 in the southwestern Pacific Basin. *Geology*, 30(1), 67-70.
- 1174 Larter, R. D., & Barker, P. F. (1991). Effects of ridge crest-trench interaction on Antarctic-  
1175 Phoenix spreading: forces on a young subducting plate. *Journal of Geophysical Research:*  
1176 *Solid Earth*, 96(B12), 19583-19607.
- 1177 Larter, R. D., Cunningham, A. P., Barker, P. F., Gohl, K., & Nitsche, F. O. (2002). Tectonic evolution  
1178 of the Pacific margin of Antarctica 1. Late Cretaceous tectonic reconstructions. *Journal of*  
1179 *Geophysical Research: Solid Earth*, 107(B12), EPM-5.  
1180 <https://doi.org/10.1029/2000JB000052>
- 1181 Lawver, L. A., & Gahagan, L. M. (1994). Constraints on timing of extension in the Ross Sea  
1182 region. *Terra Antartica*, 1(3), 545-552.
- 1183 Li, H., Ling, M. X., Li, C. Y., Zhang, H., Ding, X., Yang, X. Y., ... & Sun, W. D. (2012). A-type granite  
1184 belts of two chemical subgroups in central eastern China: Indication of ridge  
1185 subduction. *Lithos*, 150, 26-36.
- 1186 Llubes, M., Seoane, L., Bruinsma, S., & Rémy, F. (2018). Crustal thickness of Antarctica estimated  
1187 using data from gravimetric satellites. *Solid Earth*, 9(2), 457-467.
- 1188 Loiselle, M.C., and Wones, D.R., 1979, Characteristics and origin of anorogenic granites:  
1189 Geological Society of America Abstracts with Programs, v. 11, p. 468.
- 1190 Luyendyk, B. P. (1995). Hypothesis for Cretaceous rifting of east Gondwana caused by  
1191 subducted slab capture. *Geology*, 23(4), 373-376. [https://doi.org/10.1130/0091-](https://doi.org/10.1130/0091-7613(1995)023<0373:HFCROE>2.3.CO;2)  
1192 [7613\(1995\)023<0373:HFCROE>2.3.CO;2](https://doi.org/10.1130/0091-7613(1995)023<0373:HFCROE>2.3.CO;2)
- 1193 Mahoney, J. J., Storey, M., Duncan, R. A., Spencer, K. J., & Pringle, M. (1993). Geochemistry and age  
1194 of the Ontong Java Plateau. *The Mesozoic Pacific: Geology, Tectonics, and Volcanism*,  
1195 *Geophys. Monogr. Ser.*, 77, 233-261.
- 1196 Matthews, K. J., Müller, R. D., Wessel, P., & Whittaker, J. M. (2011). The tectonic fabric of the  
1197 ocean basins. *Journal of Geophysical Research: Solid Earth*, 116(B12).

- 1198 Matthews, K. J., Seton, M., & Müller, R. D. (2012). A global-scale plate reorganization event at  
1199 105–100 Ma. *Earth and Planetary Science Letters*, 355, 283-298.  
1200 <https://doi.org/10.1016/j.epsl.2012.08.023>
- 1201 Matthews, K. J., Williams, S. E., Whittaker, J. M., Müller, R. D., Seton, M., & Clarke, G. L. (2015).  
1202 Geologic and kinematic constraints on Late Cretaceous to mid Eocene plate boundaries in  
1203 the southwest Pacific. *Earth-Science Reviews*, 140, 72-107.
- 1204 Maurizot, P., Cluzel, D., Patriat, M., Collot, J., Iseppi, M., Lesimple, S., Sechiari, A., Bosch, D.,  
1205 Montanini, A., Macera, P., & Davies, H. L. (2020a). The Eocene subduction–obduction  
1206 complex of New Caledonia. *Geological Society, London, Memoirs*, 51(1), 93-130.
- 1207 Maurizot, P., Cluzel, D., Meffre, S., Campbell, H. J., Collot, J., & Sevin, B. (2020b). Pre-Late  
1208 Cretaceous basement terranes of the Gondwana active margin of New  
1209 Caledonia. *Geological Society, London, Memoirs*, 51(1), 27-52.
- 1210 Mazengarb, C., & Harris, D. H. M. (1994). Cretaceous stratigraphic and structural relations of  
1211 Raukumara Peninsula, New Zealand: stratigraphic patterns associated with the migration  
1212 of a thrust system. In *Annales Tectonicae* (Vol. 8, pp. 100-118).
- 1213 McCarron, J. J., & Larter, R. D. (1998). Late Cretaceous to early Tertiary subduction history of the  
1214 Antarctic Peninsula. *Journal of the Geological Society*, 155(2), 255-268.
- 1215 McCarthy, A., Magri, L., Sauermilch, I., Fox, J., Seton, M., Mohn, G., Tugend, J., Feig, S., Falloon, T., &  
1216 Whittaker, J. M. The Louisiade ophiolite: a missing link in the western Pacific. *Terra Nova*.
- 1217 Molnar, P., Atwater, T., Mammerickx, J., & Smith, S. M. (1975). Magnetic anomalies, bathymetry  
1218 and the tectonic evolution of the South Pacific since the Late Cretaceous. *Geophysical  
1219 Journal International*, 40(3), 383-420.
- 1220 Mortimer, N. (2004). New Zealand's geological foundations. *Gondwana research*, 7(1), 261-272.
- 1221 Mortimer, N., Hoernle, K., Hauff, F., Palin, J. M., Dunlap, W. J., Werner, R., & Faure, K. (2006). New  
1222 constraints on the age and evolution of the Wishbone Ridge, southwest Pacific Cretaceous  
1223 microplates, and Zealandia–West Antarctica breakup. *Geology*, 34(3), 185-188.
- 1224 Mortimer, N., Rattenbury, M. S., King, P. R., Bland, K. J., Barrell, D. J. A., Bache, F., Begg, J. G.,  
1225 Campbell, H. J., Cox, S. C., Crampton, J. S., Edbrooke, S. W., Forsyth, P. J., Johnston, M. R.,  
1226 Jongens, R., Lee, J. M., Leonard, G. S., Raine, J. I., Skinner, D. N. B., Timm, C., Townsend, D. B.,  
1227 Tulloch, A. J., Turnbull, I. M., & Turnbull, R. E. (2014). High-level stratigraphic scheme for  
1228 New Zealand rocks. *New Zealand Journal of Geology and Geophysics*, 57(4), 402-419.
- 1229 Mortimer, N., Campbell, H. J., Tulloch, A. J., King, P. R., Stagpoole, V. M., Wood, R. A., Rattenbury,  
1230 M.S., Sutherland, R., Adams, C. J., Collot, J. & Seton, M. (2017). Zealandia: Earth's hidden  
1231 continent. *GSA today*, 27(3), 27-35.

- 1232 Mortimer, N., van den Bogaard, P., Hoernle, K., Timm, C., Gans, P. B., Werner, R., & Riefstahl, F.  
1233 (2019). Late Cretaceous oceanic plate reorganization and the breakup of Zealandia and  
1234 Gondwana. *Gondwana Research*, 65, 31-42. <https://doi.org/10.1016/j.gr.2018.07.010>
- 1235 Mueller, C. O., & Jokat, W. (2019). The initial Gondwana break-up: a synthesis based on new  
1236 potential field data of the Africa-Antarctica Corridor. *Tectonophysics*, 750, 301-328.
- 1237 Müller, R. D., Cannon, J., Qin, X., Watson, R. J., Gurnis, M., Williams, S., Pfaffelmoser, T., Seton, M.,  
1238 Russel, S. H. J., & Zahirovic, S. (2018). GPlates: building a virtual Earth through deep  
1239 time. *Geochemistry, Geophysics, Geosystems*, 19(7), 2243-2261.
- 1240 Müller, R. D., Zahirovic, S., Williams, S. E., Cannon, J., Seton, M., Bower, D. J., Tetley, M. G., Heine,  
1241 C., Le Breton, E., Liu, S., Russel, S. H. J., Yang, T., Leonard, J., & Gurnis, M. (2019). A global  
1242 plate model including lithospheric deformation along major rifts and orogens since the  
1243 Triassic. *Tectonics*, 38(6), 1884-1907. <https://doi.org/10.1029/2018TC005462>
- 1244 Muir, R. J., Ireland, T. R., Weaver, S. D., Bradshaw, J. D., Waight, T. E., Jongens, R., & Eby, G. N.  
1245 (1997). SHRIMP U-Pb geochronology of Cretaceous magmatism in northwest Nelson-  
1246 Westland, South Island, New Zealand. *New Zealand Journal of Geology and*  
1247 *Geophysics*, 40(4), 453-463. <https://doi.org/10.1080/00288306.1997.9514775>
- 1248 Nakanishi, M., Tamaki, K., & Kobayashi, K. (1992). Magnetic anomaly lineations from Late  
1249 Jurassic to Early Cretaceous in the west-central Pacific Ocean. *Geophysical Journal*  
1250 *International*, 109(3), 701-719.
- 1251 Nakanishi, M., & Winterer, E. L. (1998). Tectonic history of the Pacific-Farallon-Phoenix triple  
1252 junction from Late Jurassic to Early Cretaceous: an abandoned Mesozoic spreading system  
1253 in the central Pacific basin. *Journal of Geophysical Research: Solid Earth*, 103(B6), 12453-  
1254 12468.
- 1255 NOAA National Geophysical Data Center (2009). ETOPO1 1 Arc-Minute Global Relief Model.  
1256 NOAA National Centers for Environmental Information.
- 1257 O'Neill, C., Müller, D., & Steinberger, B. (2005). On the uncertainties in hot spot reconstructions  
1258 and the significance of moving hot spot reference frames. *Geochemistry, Geophysics,*  
1259 *Geosystems*, 6(4).
- 1260 Ogg, J. G. (2020). Geomagnetic polarity time scale  
1261 In F.M. Gradstein, J.G. Ogg, M.D. Schmitz, G.M. Ogg (Eds.), *Geologic Time Scale*  
1262 *2020*, Elsevier, Amsterdam (2020), pp. 159-192,
- 1263 Pepper, M., Gehrels, G., Pullen, A., Ibanez-Mejia, M., Ward, K. M., & Kapp, P. (2016). Magmatic  
1264 history and crustal genesis of western South America: Constraints from U-Pb ages and Hf  
1265 isotopes of detrital zircons in modern rivers. *Geosphere*, 12(5), 1532-1555.
- 1266 Petterson, M. G., Neal, C. R., Mahoney, J. J., Kroenke, L. W., Saunders, A. D., Babbs, T. L., Duncan, R.  
1267 A., Tolia, D., & McGrail, B. (1997). Structure and deformation of north and central Malaita,

- 1268 Solomon Islands: tectonic implications for the Ontong Java Plateau-Solomon arc collision,  
1269 and for the fate of oceanic plateaus. *Tectonophysics*, 283(1-4), 1-33.
- 1270 Pindell, J.L. and Kennan, L. (2009). Tectonic evolution of the Gulf of Mexico, Caribbean and  
1271 northern South America in the mantle reference frame: an update. Geological Society,  
1272 London, Special Publications, 328(1): 1.1-55.
- 1273 Qayyum, A., Lom, N., Advokaat, E.L., Spakman, W., van der Meer, D.G. and van Hinsbergen, D.J.J.  
1274 (2022). Subduction and slab detachment under moving trenches during ongoing India-  
1275 Asia convergence. *Earth and Space Science Open Archive*: 45.
- 1276 Quarles van Ufford, A., & Cloos, M. (2005). Cenozoic tectonics of New Guinea. *AAPG*  
1277 *bulletin*, 89(1), 119-140.
- 1278 Raza, A., Hill, K. C., & Korsch, R. J. (2009). Mid-Cretaceous uplift and denudation of the Bowen  
1279 and Surat Basins, eastern Australia: relationship to Tasman Sea rifting from apatite  
1280 fission-track and vitrinite-reflectance data. *Australian Journal of Earth Sciences*, 56(3),  
1281 501-531.
- 1282 Rey, P., Müller, R. (2010) Fragmentation of active continental plate margins owing to the  
1283 buoyancy of the mantle wedge. *Nature Geosci* 3, 257–261.  
1284 <https://doi.org/10.1038/ngeo825>
- 1285 Reyners, M., Eberhart-Phillips, D., & Bannister, S. (2011). Tracking repeated subduction of the  
1286 Hikurangi Plateau beneath New Zealand. *Earth and Planetary Science Letters*, 311(1-2),  
1287 165-171.
- 1288 Reyners, M., Eberhart-Phillips, D., Upton, P., & Gubbins, D. (2017). Three-dimensional imaging of  
1289 impact of a large igneous province with a subduction zone. *Earth and Planetary Science*  
1290 *Letters*, 460, 143-151.
- 1291 Riefstahl, F., Gohl, K., Davy, B., Hoernle, K., Mortimer, N., Timm, C., Werner, R., & Hochmuth, K.  
1292 (2020). Cretaceous intracontinental rifting at the southern Chatham Rise margin and  
1293 initialisation of seafloor spreading between Zealandia and Antarctica. *Tectonophysics*, 776,  
1294 228298.
- 1295 Schellart, W. P., Lister, G. S., & Toy, V. G. (2006). A Late Cretaceous and Cenozoic reconstruction  
1296 of the Southwest Pacific region: tectonics controlled by subduction and slab rollback  
1297 processes. *Earth-Science Reviews*, 76(3-4), 191-233.
- 1298 Sdrolias, M., Müller, R. D., & Gaina, C. (2003). Tectonic evolution of the southwest Pacific using  
1299 constraints from backarc basins. *Geological Society of America Special Papers*, 372, 343–  
1300 359.
- 1301 Seton, M., Müller, R. D., Zahirovic, S., Gaina, C., Torsvik, T., Shephard, G., Talsma, A., Gurnis, M.,  
1302 Maus, S., & Chandler, M. (2012). Global continental and ocean basin reconstructions since

- 1303 200 Ma. *Earth-Science Reviews*, 113(3-4), 212-270.
- 1304 <https://doi.org/10.1016/j.earscirev.2012.03.002>
- 1305 Seton, M., Whittaker, J. M., Wessel, P., Müller, R. D., DeMets, C., Merkouriev, S., Cande, S., Eagles,  
1306 G., Granot, R., Stock, J., Wright, N., Williams, S. E. (2014). Community infrastructure and  
1307 repository for marine magnetic identifications. *Geochemistry, Geophysics,*  
1308 *Geosystems*, 15(4), 1629-1641.
- 1309 Shapiro, M. N., & Solov'ev, A. V. (2009). Formation of the Olyutorsky–Kamchatka foldbelt: A  
1310 kinematic model. *Russian Geology and Geophysics*, 50(8), 668-681.
- 1311 Shen, W., Wiens, D. A., Anandkrishnan, S., Aster, R. C., Gerstoft, P., Bromirski, P. D., Hansen, S. E.,  
1312 Dalziel, I. W. D., Heeszel, D. S., Huerta, A. D., Nyblade, A. A., Stephen, R., Wilson, T. J., &  
1313 Winberry, J. P. (2018). The crust and upper mantle structure of central and West  
1314 Antarctica from Bayesian inversion of Rayleigh wave and receiver functions. *Journal of*  
1315 *Geophysical Research: Solid Earth*, 123(9), 7824-7849.
- 1316 Sliter, W. V., Ishizaki, K., & Saito, T. (1992). Cretaceous planktonic foraminiferal biostratigraphy  
1317 and paleoceanographic events in the Pacific Ocean with emphasis on indurated  
1318 sediment. *Centenary of Japanese Micropaleontology*, 281-99.
- 1319 Smith, T. R., & Cole, J. W. (1997). Somers ignimbrite formation: Cretaceous high-grade  
1320 ignimbrites from South Island, New Zealand. *Journal of Volcanology and Geothermal*  
1321 *Research*, 75(1-2), 39-57.
- 1322 Spiegel, C., Lindow, J., Kamp, P. J., Meisel, O., Mukasa, S., Lisker, F., Kuhn, G., & Gohl, K. (2016).  
1323 Tectonomorphic evolution of Marie Byrd Land–Implications for Cenozoic rifting activity  
1324 and onset of West Antarctic glaciation. *Global and Planetary Change*, 145, 98-115.
- 1325 Steinberger, B., Sutherland, R., & O'Connell, R. J. (2004). Prediction of Emperor-Hawaii seamount  
1326 locations from a revised model of global plate motion and mantle flow. *Nature*, 430(6996),  
1327 167-173.
- 1328 Stock, J. M., & Cande, S. C. (2002). Tectonic history of Antarctic seafloor in the Australia-New  
1329 Zealand-South Pacific sector: Implications for Antarctic continental tectonics.
- 1330 Stock, J., & Molnar, P. (1987). Revised history of early Tertiary plate motion in the south-west  
1331 Pacific. *Nature*, 325(6104), 495-499.
- 1332 Sutherland, R., & Hollis, C. (2001). Cretaceous demise of the Moa plate and strike-slip motion at  
1333 the Gondwana margin. *Geology*, 29(3), 279-282.
- 1334 Taylor, B. (2006). The single largest oceanic plateau: Ontong Java–Manihiki–Hikurangi. *Earth*  
1335 *and Planetary Science Letters*, 241(3-4), 372-380.
- 1336 Tebbens, S. F., & Cande, S. C. (1997). Southeast Pacific tectonic evolution from early Oligocene to  
1337 present. *Journal of Geophysical Research: Solid Earth*, 102(B6), 12061-12084.

- 1338 Tebbens, S. F., Cande, S. C., Kovacs, L., Parra, J. C., LaBrecque, J. L., & Vergara, H. (1997). The Chile  
1339 ridge: A tectonic framework. *Journal of Geophysical Research: Solid Earth*, *102*(B6), 12035-  
1340 12059.
- 1341 Timm, C., Hoernle, K., Werner, R., Hauff, F., van den Bogaard, P., Michael, P., Coffin, M. F., &  
1342 Koppers, A. (2011). Age and geochemistry of the oceanic Manihiki Plateau, SW Pacific:  
1343 New evidence for a plume origin. *Earth and Planetary Science Letters*, *304*(1-2), 135-146.
- 1344 Torsvik, T. H., Müller, R. D., Van der Voo, R., Steinberger, B., & Gaina, C. (2008). Global plate  
1345 motion frames: toward a unified model. *Reviews of geophysics*, *46*(3).
- 1346 Torsvik, T. H., Steinberger, B., Shephard, G. E., Doubrovine, P. V., Gaina, C., Domeier, M., Conrad,  
1347 C. P., & Sager, W. W. (2019). Pacific-Panthalassic reconstructions: Overview, errata and  
1348 the way forward. *Geochemistry, Geophysics, Geosystems*, *20*(7), 3659-3689.  
1349 <https://doi.org/10.1029/2019GC008402>
- 1350 Tulloch, A. J., & Kimbrough, D. L. (1989). The Paparoa metamorphic core complex, New Zealand:  
1351 cretaceous extension associated with fragmentation of the Pacific margin of  
1352 Gondwana. *Tectonics*, *8*(6), 1217-1234.
- 1353 Tulloch, A. J., Kimbrough, D. L., Landis, C. A., Mortimer, N., & Johnston, M. R. (1999).  
1354 Relationships between the Brook Street terrane and Median Tectonic Zone (Median  
1355 batholith): evidence from Jurassic conglomerates. *New Zealand Journal of Geology and  
1356 Geophysics*, *42*(2), 279-293.
- 1357 Tulloch, A. J., & Rabone, S. D. C. (1993). Mo-bearing granodiorite porphyry plutons of the Early  
1358 Cretaceous Separation Point Suite, west Nelson, New Zealand. *New Zealand journal of  
1359 geology and geophysics*, *36*(4), 401-408.
- 1360 Tulloch A. J. & Kimbrough D. L. (2003) in *Tectonic Evolution of Northwestern Mexico and the  
1361 Southwestern USA*, Paired plutonic belts in convergent margins and the development of  
1362 high Sr/Y magmatism: Peninsular Ranges batholith of Baja-California and Median  
1363 batholith of New Zealand, Geological Society of America Special Papers, eds Johnson S.  
1364 E., Paterson S. R., Fletcher J. M., Girty G. H., Kimbrough D. L., Martín-Barajas A. 374,  
1365 pp 275–295
- 1366 Tulloch, A. J., Ramezani, J., Mortimer, N., Mortensen, J., van den Bogaard, P., & Maas, R. (2009).  
1367 Cretaceous felsic volcanism in New Zealand and Lord Howe Rise (Zealandia) as a  
1368 precursor to final Gondwana break-up. *Geological Society, London, Special  
1369 Publications*, *321*(1), 89-118. <https://doi.org/10.1144/SP321.5>
- 1370 Vaes, B., Van Hinsbergen, D. J. J., & Boschman, L. M. (2019). Reconstruction of subduction and  
1371 back-arc spreading in the NW Pacific and Aleutian Basin: Clues to causes of Cretaceous  
1372 and Eocene plate reorganizations. *Tectonics*, *38*(4), 1367-1413.

- 1373 Van de Lagemaat, S. H.A, Van Hinsbergen, D. J. J., Boschman, L. M., Kamp, P. J. J., & Spakman, W.  
1374 (2018a). Southwest Pacific absolute plate kinematic reconstruction reveals major  
1375 Cenozoic Tonga-Kermadec slab dragging. *Tectonics*, 37(8), 2647-2674.
- 1376 Van de Lagemaat, S. H.A, Boschman, L. M., Kamp, P. J. J., Langereis, C. G., & van Hinsbergen, D. J. J.  
1377 (2018b). Post-remagnetisation vertical axis rotation and tilting of the Murihiku Terrane  
1378 (North Island, New Zealand). *New Zealand Journal of Geology and Geophysics*, 61(1), 9-25.
- 1379 Van de Lagemaat, S. H. A., Swart, M. L., Vaes, B., Kosters, M. E., Boschman, L. M., Burton-Johnson,  
1380 A., Bijl, P. K., Spakman, W., & Van Hinsbergen, D. J. J. (2021). Subduction initiation in the  
1381 Scotia Sea region and opening of the Drake Passage: When and why?. *Earth-Science*  
1382 *Reviews*, 215, 103551.
- 1383 Van Der Meer, D. G., Spakman, W., Van Hinsbergen, D. J., Amaru, M. L., & Torsvik, T. H. (2010).  
1384 Towards absolute plate motions constrained by lower-mantle slab remnants. *Nature*  
1385 *Geoscience*, 3(1), 36-40.
- 1386 Van der Meer, Q. H., Storey, M., Scott, J. M., & Waight, T. E. (2016). Abrupt spatial and  
1387 geochemical changes in lamprophyre magmatism related to Gondwana fragmentation  
1388 prior, during and after opening of the Tasman Sea. *Gondwana Research*, 36, 142-156.  
1389 <https://doi.org/10.1016/j.gr.2016.04.004>
- 1390 Van der Meer, Q. H. A., Waight, T. E., Scott, J. M., & Münker, C. (2017). Variable sources for  
1391 Cretaceous to recent HIMU and HIMU-like intraplate magmatism in New Zealand. *Earth*  
1392 *and Planetary Science Letters*, 469, 27-41. <https://doi.org/10.1016/j.epsl.2017.03.037>
- 1393 Van Der Meer, Q. H. A., Waight, T. E., Tulloch, A. J., Whitehouse, M. J., & Andersen, T. (2018).  
1394 Magmatic evolution during the Cretaceous transition from subduction to continental  
1395 break-up of the Eastern Gondwana margin (New Zealand) documented by in-situ zircon  
1396 O-Hf isotopes and bulk-rock Sr-Nd isotopes. *Journal of Petrology*, 59(5), 849-880.  
1397 <https://doi.org/10.1093/petrology/egy047>
- 1398 Van Hinsbergen, D. J., & Schouten, T. L. (2021). Deciphering paleogeography from orogenic  
1399 architecture: constructing orogens in a future supercontinent as thought  
1400 experiment. *American Journal of Science*, 321(6), 955-1031.
- 1401 Van Hunen, J. and Allen, M.B., 2011. Continental collision and slab break-off: A comparison of 3-  
1402 D numerical models with observations. *Earth and Planetary Science Letters*, 302(1-2): 27-  
1403 37.
- 1404 Veevers, J. J. (2012). Reconstructions before rifting and drifting reveal the geological  
1405 connections between Antarctica and its conjugates in Gondwanaland. *Earth-Science*  
1406 *Reviews*, 111(3-4), 249-318.

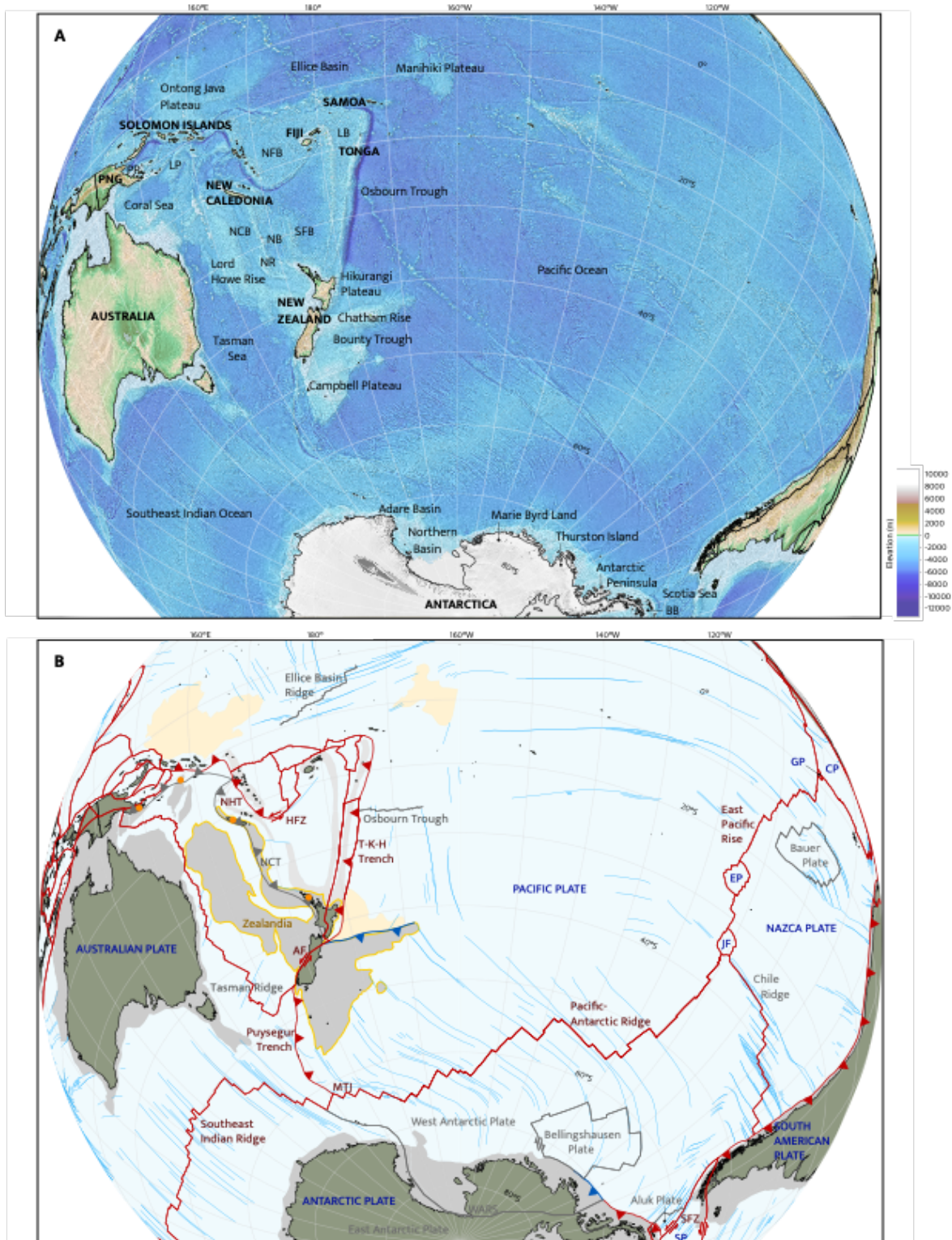


- 1407 Villamor, P., & Berryman, K. (2001). A late Quaternary extension rate in the Taupo Volcanic  
1408 Zone, New Zealand, derived from fault slip data. *New Zealand Journal of Geology and*  
1409 *Geophysics*, 44(2), 243-269.
- 1410 Viso, R. F., Larson, R. L., & Pockalny, R. A. (2005). Tectonic evolution of the Pacific–Phoenix–  
1411 Farallon triple junction in the South Pacific Ocean. *Earth and Planetary Science*  
1412 *Letters*, 233(1-2), 179-194.
- 1413 Waight, T. E., Weaver, S. D., & Muir, R. J. (1998). Mid-Cretaceous granitic magmatism during the  
1414 transition from subduction to extension in southern New Zealand: a chemical and tectonic  
1415 synthesis. *Lithos*, 45(1-4), 469-482. [https://doi.org/10.1016/S0024-4937\(98\)00045-0](https://doi.org/10.1016/S0024-4937(98)00045-0)
- 1416 Webb, A.A.G., Guo, H., Clift, P.D., Husson, L., Müller, T., Costantino, D., Yin, A., Xu, Z., Cao, H. and  
1417 Wang, Q. (2017). The Himalaya in 3D: Slab dynamics controlled mountain building and  
1418 monsoon intensification. *Lithosphere*.
- 1419 Wessel, P., Matthews, K. J., Müller, R. D., Mazzoni, A., Whittaker, J. M., Myhill, R., & Chandler, M. T.  
1420 (2015). *Semiautomatic fracture zone tracking* (Vol. 16, No. 7, pp. 2462-2472).
- 1421 Whattam, S. A., Malpas, J., Smith, I. E., & Ali, J. R. (2006). Link between SSZ ophiolite formation,  
1422 emplacement and arc inception, Northland, New Zealand: U–Pb SHRIMP constraints;  
1423 Cenozoic SW Pacific tectonic implications. *Earth and Planetary Science Letters*, 250(3-4),  
1424 606-632.
- 1425 Whattam, S. A., Malpas, J., Ali, J. R., & Smith, I. E. (2008). New SW Pacific tectonic model: Cyclical  
1426 intraoceanic magmatic arc construction and near-coeval emplacement along the  
1427 Australia-Pacific margin in the Cenozoic. *Geochemistry, Geophysics, Geosystems*, 9(3).
- 1428 Whattam, S.A. and Stern, R.J. (2015). Late Cretaceous plume-induced subduction initiation along  
1429 the southern margin of the Caribbean and NW South America: The first documented  
1430 example with implications for the onset of plate tectonics. *Gondwana Research*, 27(1): 38-  
1431 63.
- 1432 Whittaker, J. M., Muller, R. D., Leitchenkov, G., Stagg, H., Sdrolias, M., Gaina, C., &  
1433 Goncharov, A. (2007). Major Australian-Antarctic plate reorganization at Hawaiian-  
1434 Emperor bend time. *Science*, 318(5847), 83-86.
- 1435 White, R. V., Tarney, J., Kerr, A. C., Saunders, A. D., Kempton, P. D., Pringle, M. S., & Klaver, G. T.  
1436 (1999). Modification of an oceanic plateau, Aruba, Dutch Caribbean: implications for the  
1437 generation of continental crust. *Lithos*, 46(1), 43-68.
- 1438 Whittaker, J. M., Williams, S. E., & Müller, R. D. (2013). Revised tectonic evolution of the Eastern  
1439 Indian Ocean. *Geochemistry, Geophysics, Geosystems*, 14(6), 1891-1909.
- 1440 Wilder, Douglas T., "Relative Motion History of the Pacific-Nazca (Farallon) Plates since 30  
1441 Million Years Ago" (2003). *USF Tampa Graduate Theses and Dissertations*.  
<https://digitalcommons.usf.edu/etd/1506>

- 1442 Williams, S. E., Whittaker, J. M., & Müller, R. D. (2011). Full-fit, palinspastic reconstruction of the  
1443 conjugate Australian-Antarctic margins. *Tectonics*, 30(6).
- 1444 Winterer, E. L., Lonsdale, P. F., Matthews, J. L., & Rosendahl, B. R. (1974, October). Structure and  
1445 acoustic stratigraphy of the Manihiki Plateau. In *Deep Sea Research and Oceanographic*  
1446 *Abstracts* (Vol. 21, No. 10, pp. 793-813). Elsevier.
- 1447 Wobbe, F., Gohl, K., Chambord, A., & Sutherland, R. (2012). Structure and breakup history of the  
1448 rifted margin of West Antarctica in relation to Cretaceous separation from Zealandia and  
1449 Bellingshausen plate motion. *Geochemistry, Geophysics, Geosystems*, 13(4).  
1450 <https://doi.org/10.1029/2011GC003742>
- 1451 Wortel, M.J.R. and Spakman, W., 2000. Subduction and slab detachment in the Mediterranean-  
1452 Carpathian region. *Science*, 290(5498): 1910-1917.
- 1453 Worthington, T. J., Hekinian, R., Stoffers, P., Kuhn, T., & Hauff, F. (2006). Osbourn Trough:  
1454 Structure, geochemistry and implications of a mid-Cretaceous paleosubducting ridge in the  
1455 South Pacific. *Earth and Planetary Science Letters*, 245(3-4), 685-701.
- 1456 Wright, N. M., Seton, M., Williams, S. E., & Mueller, R. D. (2016). The Late Cretaceous to recent  
1457 tectonic history of the Pacific Ocean basin. *Earth-Science Reviews*, 154, 138-173.  
1458 <https://doi.org/10.1016/j.earscirev.2015.11.015>
- 1459 Yan, C. Y., & Kroenke, L. W. (1993). A plate tectonic reconstruction of the Southwest Pacific, 0-  
1460 100 Ma. *Oceanic Drilling Program, Scientific Results*, 130, 697-709.
- 1461 Yang, T., Liu, S., Guo, P., Leng, W., & Yang, A. (2020). Yanshanian orogeny during North China's  
1462 drifting away from the trench: Implications of numerical models. *Tectonics*, 39(12),  
1463 e2020TC006350.
- 1464 Zhang, G. L., & Li, C. (2016). Interactions of the Greater Ontong Java mantle plume component  
1465 with the Osbourn Trough. *Scientific Reports*, 6(1), 1-8.
- 1466 Zhao, X. F., Zhou, M. F., Li, J. W., & Wu, F. Y. (2008). Association of Neoproterozoic A-and I-type  
1467 granites in South China: implications for generation of A-type granites in a subduction-  
1468 related environment. *Chemical Geology*, 257(1-2), 1-15.
- 1469
- 1470

1471 **Figures**

1472



1473

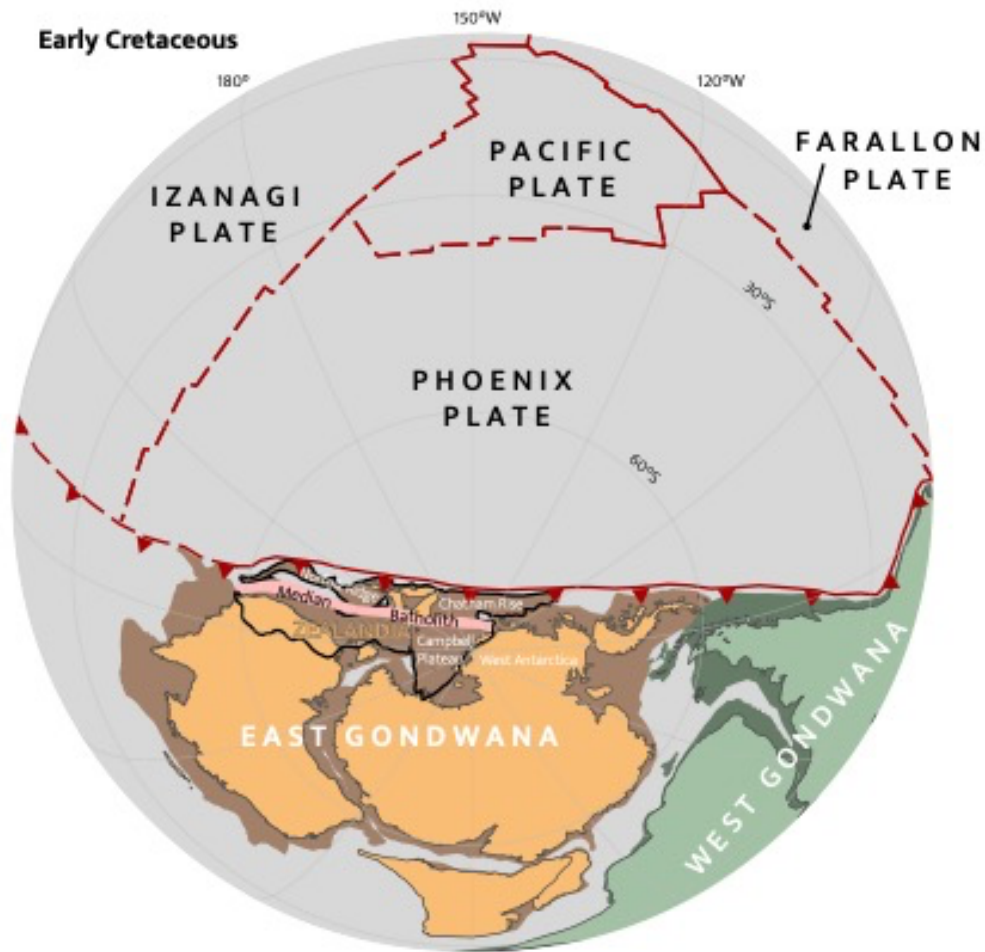
1474 **Fig. 1:** Present-day geographic and tectonic maps of the South Pacific region.

1475 **A) Geographic map**

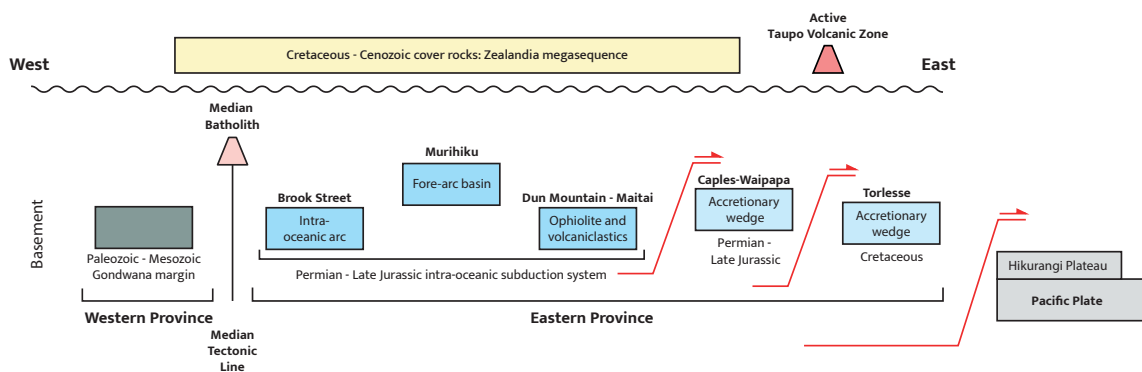
1476 BB: Bransfield Basin; LB: Lau Basin; LP: Louisiade Plateau; NB: Norfolk Basin; NCB: New  
1477 Caledonia Basin; NFB: North Fiji Basin; NR: Norfolk Ridge; PNG: Papua New Guinea; PP:  
1478 Papuan Peninsula; SFB: South Fiji Basin. Background image is ETOPO1 1 Arc-Minute Global  
1479 Relief Model. (Amante and Eakins, 2009; NOAA National Geophysical Data Center, 2009).

1480 **B) Tectonic map.** Current tectonic plate names in blue. Current plate boundaries (Bird,  
1481 2003) and plate boundary names in red, former plate names and plate boundaries in  
1482 grey, suture of East Gondwana subduction zone in blue. Continental crust of Zealandia is  
1483 outlined in yellow. Northland, New Caledonia, Louisiade, and Papuan Peninsula  
1484 ophiolites are indicated by orange dots. Ontong Java Nui Large Igneous Provinces in  
1485 light yellow. Lightblue lines are digitalized fracture zones, obtained from the GSFML  
1486 database (Matthews et al., 2011; Seton et al., 2014; Wessel et al., 2015)

1487 AF: Alpine Fault; CP: Cocos Plate; EP: Easter Plate; GP: Galapagos Plate; HFZ: Hunter  
1488 Fracture Zone; JF: Juan Fernandez Plate; MS: Manihiki Scarp; MTJ: Macquarie Triple  
1489 Junction; NHT: New Hebrides Trench; NCT: New Caledonia Trench; SFZ: Shackleton  
1490 Fracture Zone; SP: Scotia Plate; T-K-H: Tonga-Kermadec-Hikurangi; WARS: West Antarctic  
1491 Rift System.

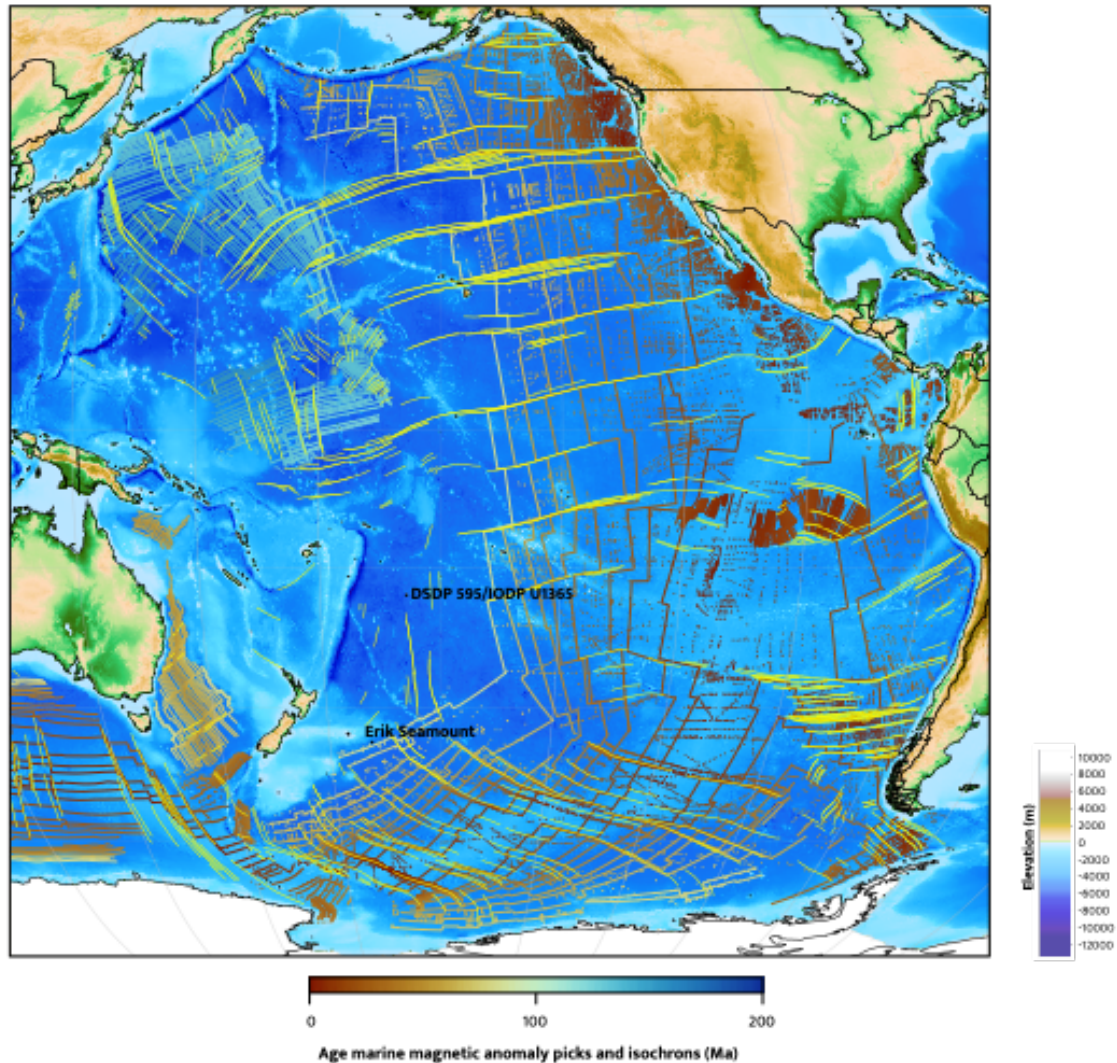


1492  
 1493 **Fig. 2:** Early Cretaceous (c. 140 Ma) reconstruction of the paleo-Pacific/Panthalassa realm  
 1494 showing the approximate extent of the Phoenix Plate. Continental crust of future Zealandia is  
 1495 outlined in black, highlighting the Zealandia margin of East Gondwana. Plate boundaries are  
 1496 only shown in the Panthalassa domain, dashed where the location of the plate boundary is  
 1497 estimated.

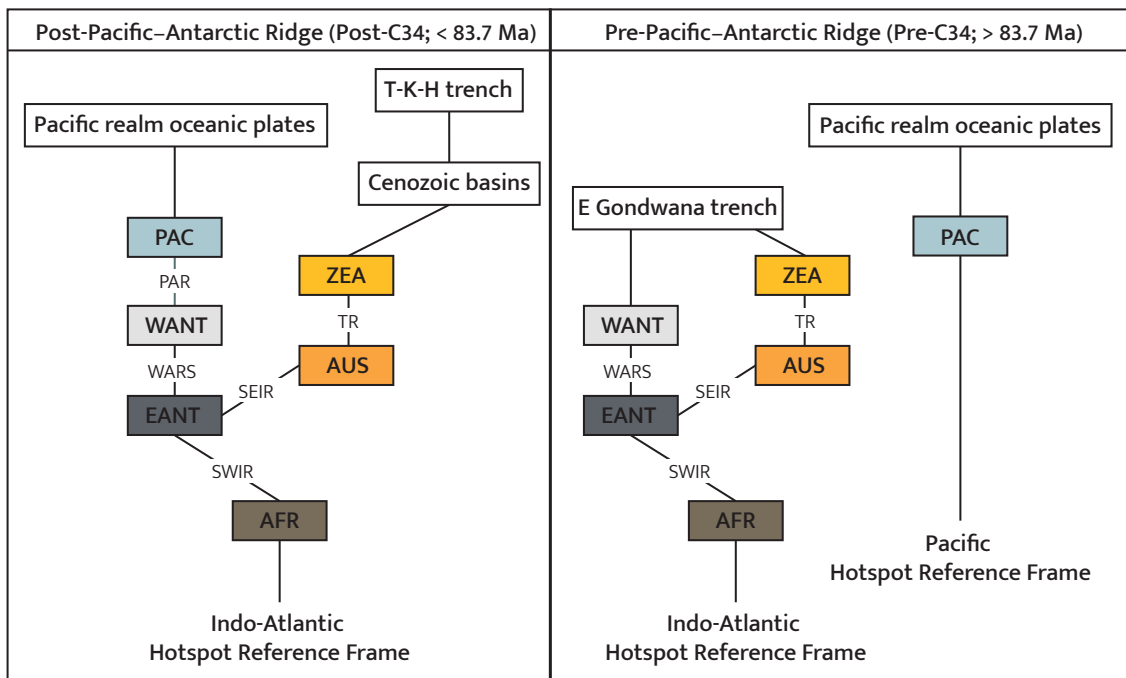


1498

1499 **Fig. 3:** Schematic cross-section of the present-day geology of the North Island of New Zealand,  
1500 based on Mortimer et al. (2014).  
1501



1502  
1503 **Fig. 4:** Geographic map of the Pacific and Southeast Indian oceans, showing the data used for the  
1504 reconstruction of the oceanic domain. Marine magnetic anomaly picks (colored by age) and  
1505 fracture zone data (in yellow) were obtained from the GSFML database (Seton et al., 2014, and  
1506 references therein). Interpreted isochrons (in white) are from Seton et al. (2012), Wright et al.  
1507 (2016), and from this study. Background image is ETOPO1 1 Arc-Minute Global Relief Model  
1508 (Amante and Eakins, 2009; NOAA National Geophysical Data Center, 2009). Marine magnetic  
1509 anomaly picks are colored using a color bar of Crameri (2018); Crameri et al. (2020)

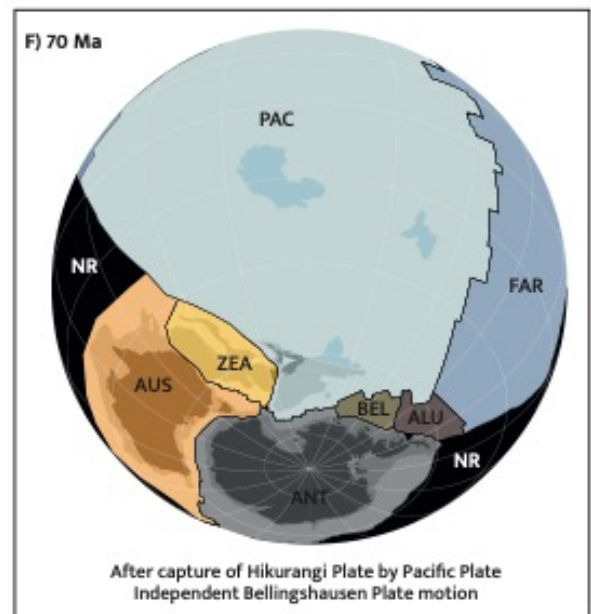
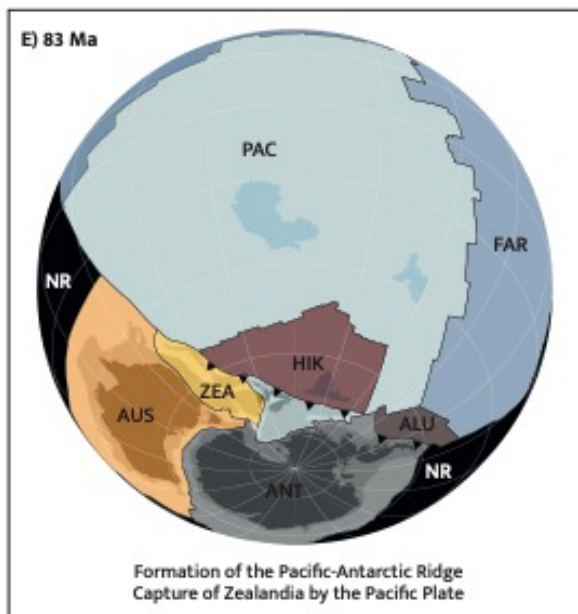
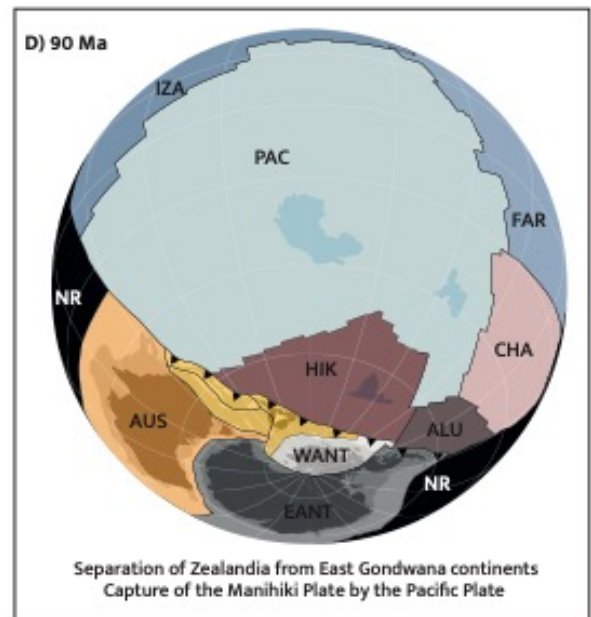
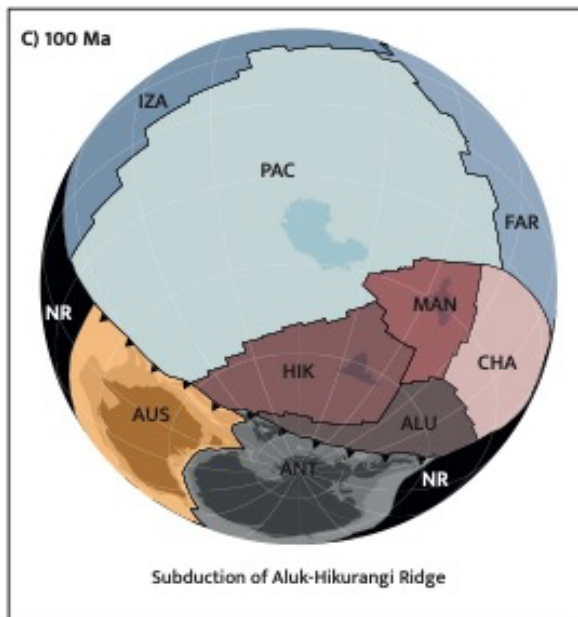
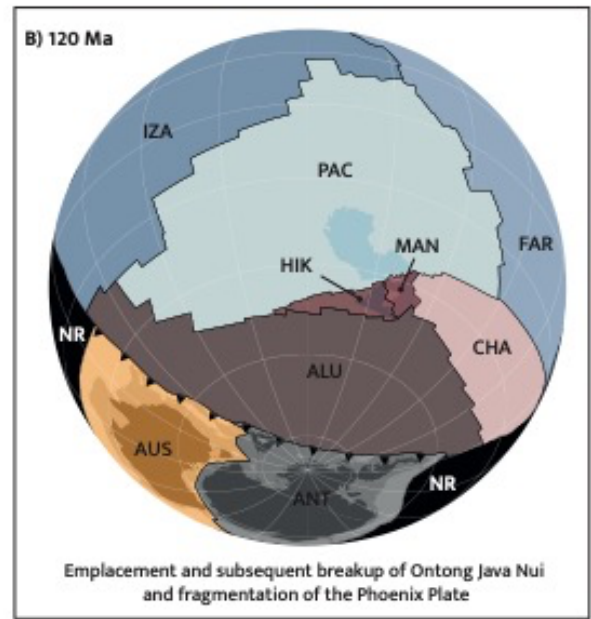
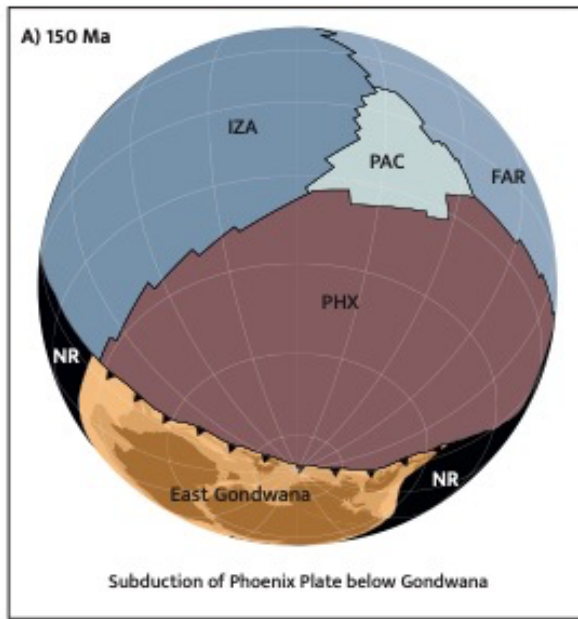


1510

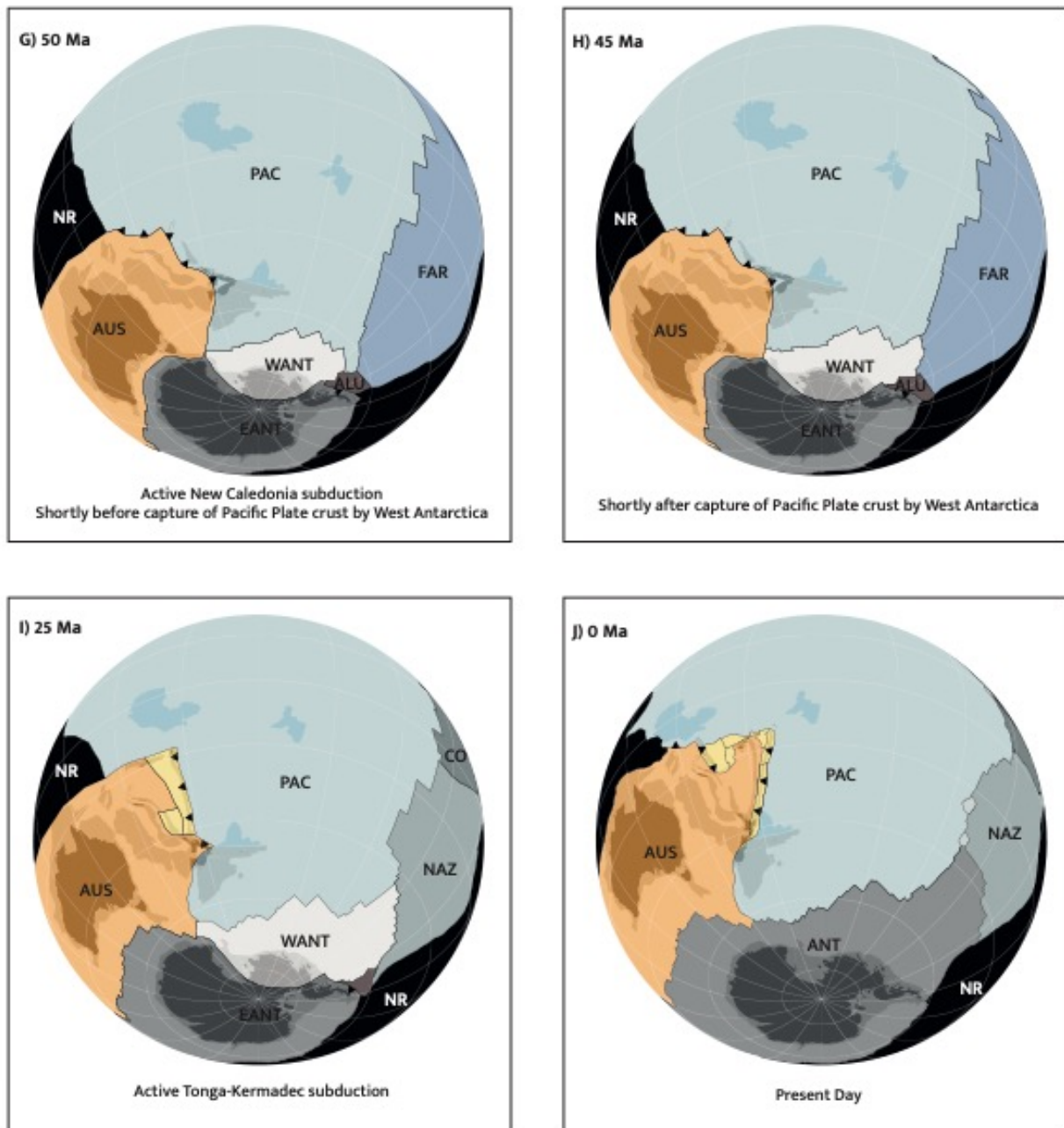
1511 **Fig. 5:** Plate circuits used in our reconstruction, highlighting the differences in the plate circuit  
 1512 before and after formation of the Pacific–Antarctic Ridge.

1513 *Plate names:* AFR: Africa; AUS: Australia; EANT: East Antarctica; WANT: West Antarctica; PAC:  
 1514 Pacific; ZEA: Zealandia;

1515 *Plate boundaries:* PAR: Pacific–Antarctic Ridge; SEIR: Southeast Indian Ridge; SWIR: Southwest  
 1516 Indian Ridge; TR: Tasman Ridge; T-K-H: Tonga–Kermadec–Hikurangi; WARS: West–Antarctic Rift  
 1517 System.







1519

1520 **Fig. 6:** Snapshots of our kinematic reconstruction in the Van der Meer (2010) reference frame,

1521 highlighting key events in the evolution of the Phoenix Plate and East Gondwana subduction

1522 zone. These events are discussed in the main text. Present-day coastlines and outline of

1523 continental crust are shaded behind the plate colors and shown for reference. The Ontong Java

1524 Nui Large Igneous Provinces are also outlined, where the outline of the Hikurangi Plateau does

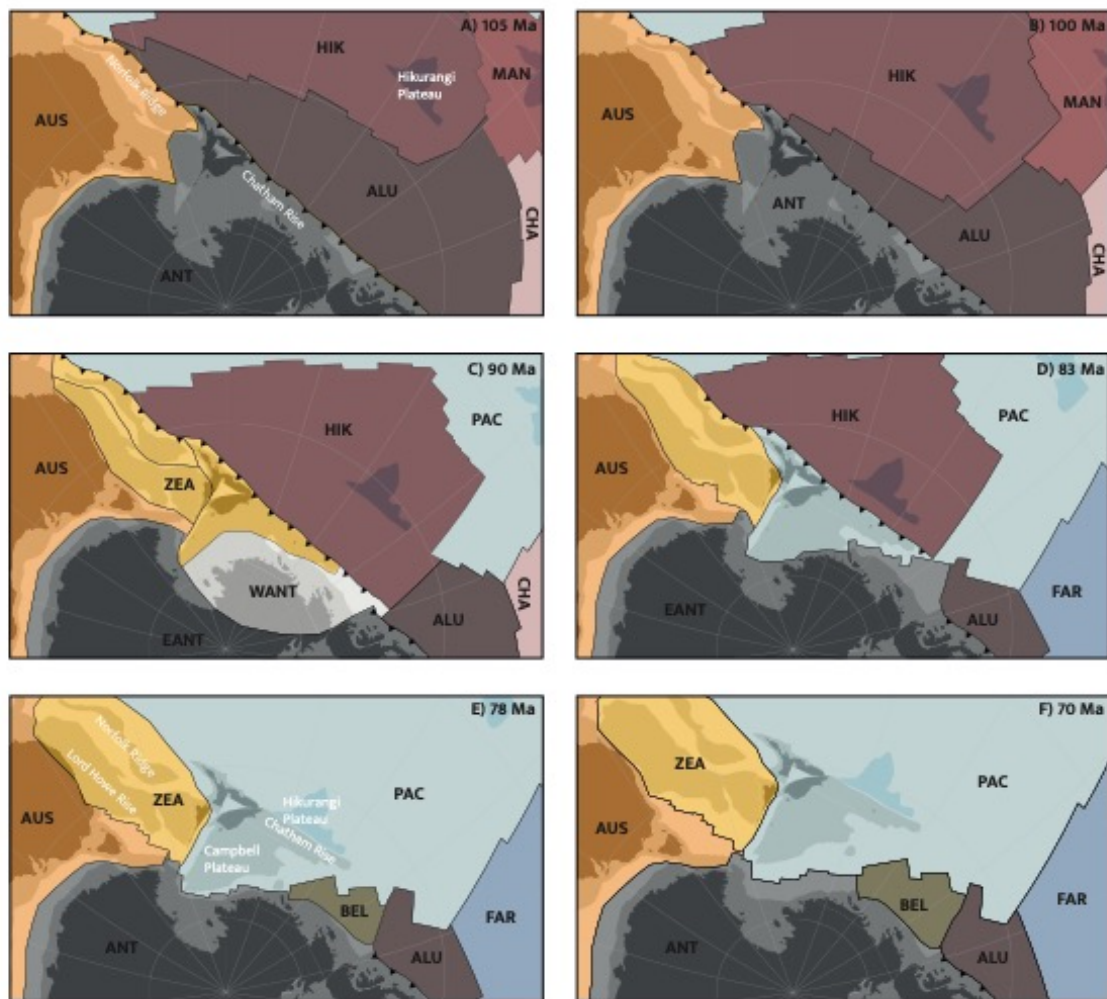
1525 not include the parts that were subducted below Chatham Rise and the North Island. Plate

1526 names: ALU: Aluk Plate; ANT: Antarctic Plate (EANT: East Antarctic Plate; WANT: West

1527 Antarctic Plate); AUS: Australian Plate; CHA: Chasca Plate; FAR: Farallon Plate; HIK: Hikurangi

1528 Plate; IZA: Izanagi Plate; MAN: Manihiki Plate; NAZ: Nazca Plate; PAC: Pacific Plate; SAM: South

1529 American Plate; ZEA: Zealandia. NR = Not Reconstructed.



1530

1531

1532

1533

1534

1535

1536

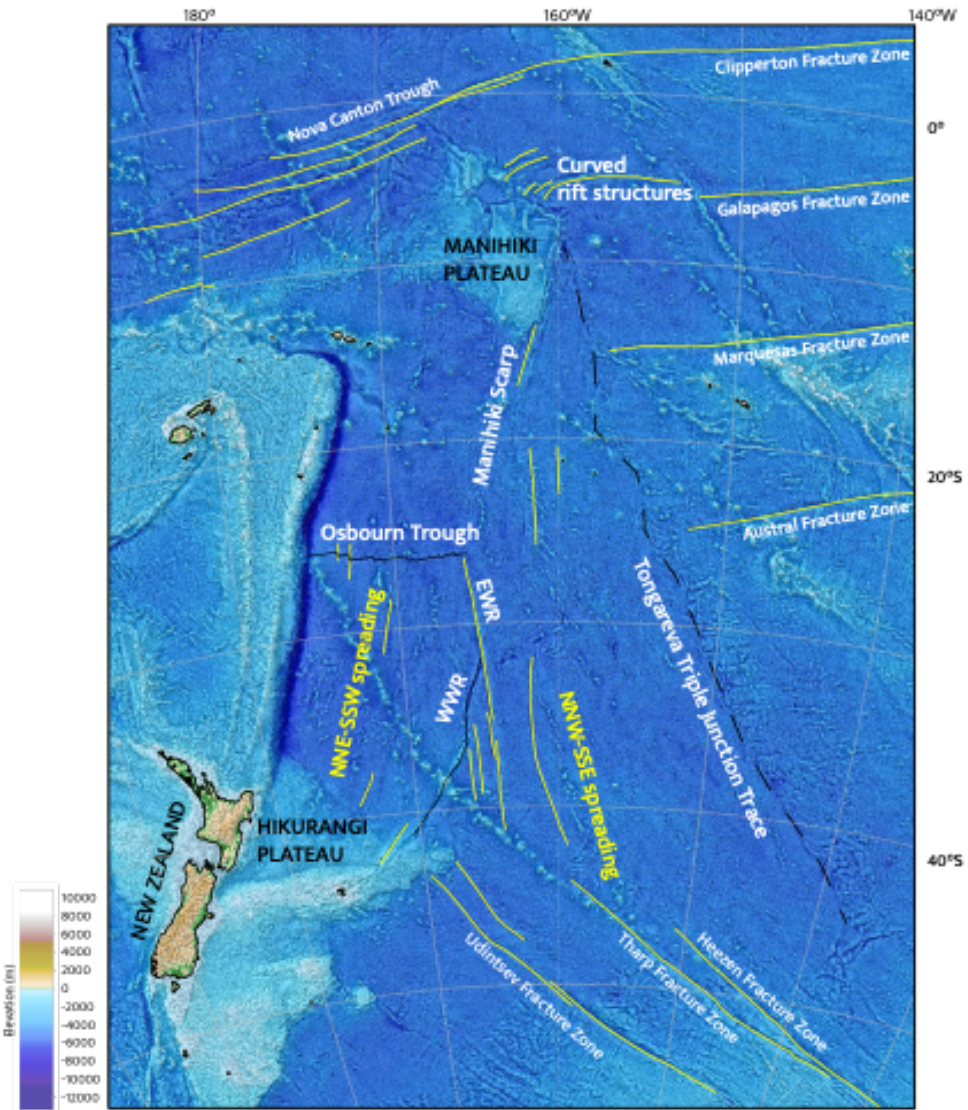
1537

1538

1539

1540

**Fig. 7:** Detailed snapshots of our kinematic reconstruction in an East Antarctica fixed reference frame, highlighting the transition from the East Gondwana subduction zone margin to a passive margin. Extension within East Gondwana started in multiple locations before subduction of the Hikurangi Plate ended and this plate as well as Zealandia became part of the Pacific plate. Present-day coastlines and outline of continental crust are shaded behind the plate colors and shown for reference. The Ontong Java Nui Large Igneous Provinces are also outlined, where the outline of the Hikurangi Plateau does not include the parts that were subducted below Chatham Rise and the North Island. Plate names: ALU: Aluk Plate; ANT: Antarctic Plate (EANT: East Antarctic Plate; WANT: West Antarctic Plate); AUS: Australian Plate; HIK: Hikurangi Plate; MAN: Manihiki Plate; NAZ: Nazca Plate; PAC: Pacific Plate; ZEA: Zealandia.



1541

1542

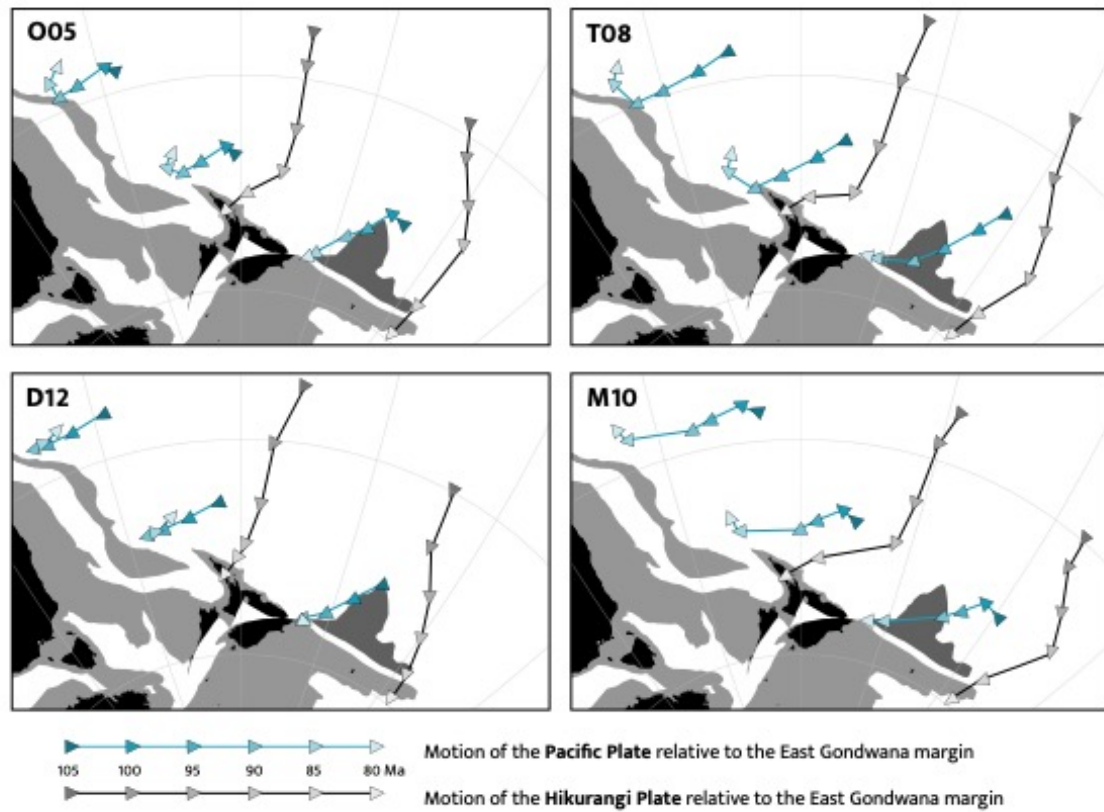
**Fig. 8:** Bathymetry of the region to the northeast of New Zealand, highlighting features of the seafloor fabric. Digitalized fracture zone data (in yellow) were obtained from the GSFML database (Matthews et al., 2011; Seton et al., 2014; Wessel et al., 2015). Background image is ETOPO1 1 Arc-Minute Global Relief Model (Amante and Eakins, 2009; NOAA National Geophysical Data Center, 2009).

1543

1544

1545

1546



1547

1548

1549

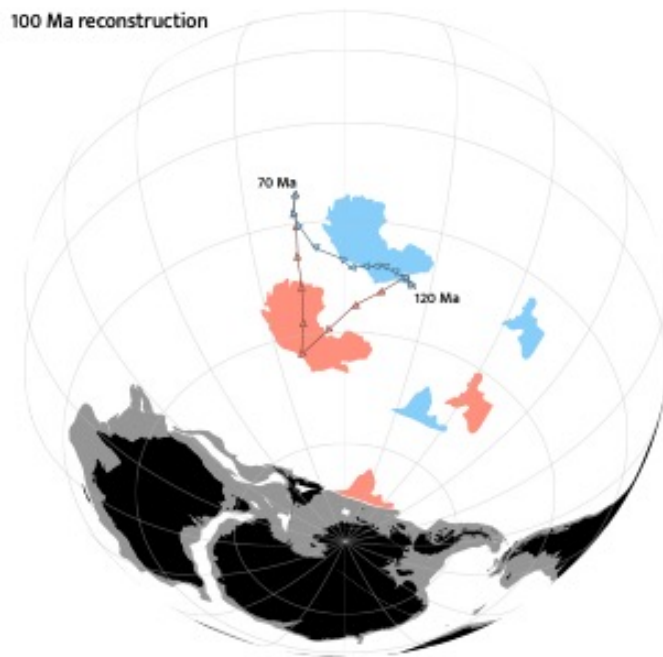
1550

1551

1552

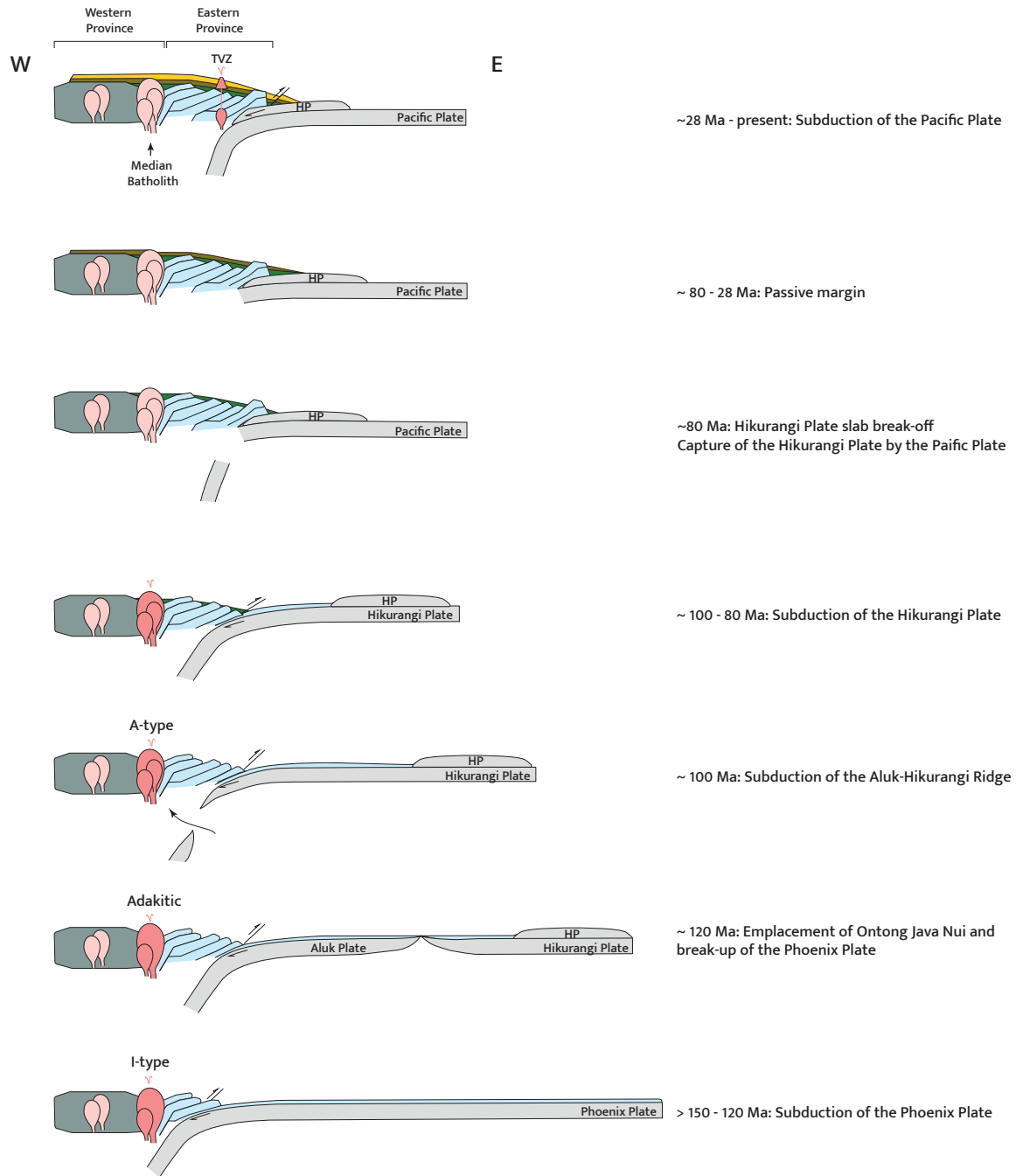
1553

**Fig. 9:** 80 Ma reconstruction in an East Antarctica fixed reference frame showing the motion of the Pacific Plate and Hikurangi Plate relative to the East Gondwana margin in different mantle reference frames (O05: O'Neill et al., 2005; T08: Torsvik et al., 2008; D12: Doubrovine et al., 2012; M10: Van der Meer et al., 2010). This figure shows that convergence between the Pacific oceanic plates and the East Gondwana margin continued until at least 90 Ma in all reference frames, and until 79 Ma if Osbourn Trough spreading was still active.



1554

1555 **Fig. 10:** 100 Ma reconstruction that shows the difference in the location of the Pacific Plate  
1556 between the hotspot reference frame of Torsvik et al. (2019) and the model of Mortimer et al.  
1557 (2019) in which the Hikurangi Plateau arrives in the East Gondwana trench at 100 Ma. The  
1558 difference is shown by the location of the LIPs, of which the Ontong Java Plateau has always  
1559 been part of the Pacific Plate. In blue is the location of the LIPs as constrained by Torsvik et al.  
1560 (2019), and in pink is the location of these plateaus in the model of Mortimer et al. (2019). Also  
1561 shown are the 120-70 Ma motion paths of the Pacific Plate that result from the two models.



1562

1563 **Fig. 11:** Schematic cross-sections along the Zealandia margin to highlight the 150 Ma to present  
 1564 tectonic history between the continental margin and the Pacific domain. The 28 Ma-present day  
 1565 cross-section is across North Island, New Zealand, where the Hikurangi Plateau is presently  
 1566 subducting, whereas older cross-sections are across the Chatham Rise where the Hikurangi  
 1567 Plateau entered the trench in the Cretaceous. TVZ refers to the active volcanism of the Taupo  
 1568 Volcanic Zone, which lies between the Waipapa and Torlesse terranes.